



Carlos Alberto Kebudi Orlando

**Optimal Wind Farm Layout Design Accounting
for Wake Effects and Contracting Strategies**

Dissertação de Mestrado

Dissertation presented to the Programa de Pós-graduação em Engenharia de Produção of PUC-Rio in partial fulfillment of the requirements for the degree of Mestre em Engenharia de Produção.

Advisor: Prof. Bruno Fânzeres dos Santos

Rio de Janeiro
October 2023



Carlos Alberto Kebudi Orlando

**Optimal Wind Farm Layout Design Accounting
for Wake Effects and Contracting Strategies**

Dissertation presented to the Programa de Pós-graduação em Engenharia de Produção of PUC-Rio in partial fulfillment of the requirements for the degree of Mestre em Engenharia de Produção. Approved by the Examination Committee.

Prof. Bruno Fânzeres dos Santos

Advisor

Departamento de Engenharia Industrial – PUC-Rio

Prof. Paula Medina Maçaira Louro

Departamento de Engenharia Industrial – PUC-Rio

Prof. João Alberto Passos Filho

UFJF

Rio de Janeiro, October 17th, 2023

All rights reserved.

Carlos Alberto Kebudi Orlando

Bachelor of Economics graduate from UFRJ in 2017, with subsequent experience in various sectors of the industry. During my master's program, I completed a summer internship in Israel with a company in the energy sector and participated in a Research and Development (R&D) project within the same industry, focusing on energy trading.

Bibliographic data

Orlando, Carlos Alberto Kebudi

Optimal wind farm layout design accounting for wake effects and contracting strategies / Carlos Alberto Kebudi Orlando ; advisor: Bruno Fânzeres dos Santos. – 2023.
56 f. : il. color. ; 30 cm

Dissertação (mestrado)–Pontifícia Universidade Católica do Rio de Janeiro, Departamento de Engenharia Industrial, 2023.

Inclui bibliografia

1. Engenharia Industrial – Teses. 2. Otimização de parque eólico. 3. Bastankhah Wake Model. 4. Conditional Value at Risk. 5. Economia da energia. 6. Estratégias de contrato. I. Santos, Bruno Fânzeres dos. II. Pontifícia Universidade Católica do Rio de Janeiro. Departamento de Engenharia Industrial. III. Título.

CDD: 658.5

Acknowledgments

I would like to express my sincere gratitude to the following individuals and organizations who contributed to the completion of this research:

- My advisor, Bruno Fânzeres, for your unwavering support and guidance, which were crucial for the success of this dissertation.
- My lab colleagues: Rafaela Ribeiro, Andrew Rosemberg, Carolina Blank, Felipe Piancó, Felipe Whitaker and João Pedro Mattos for enriching my academic journey with their ideas and experiences.
- My family and friends for their unwavering support and love.
- This study was financed in part by the Coordenação de Aperfeiçoamento de Pessoal de Nível Superior - Brasil (CAPES) - Finance Code 001.
- Other funding sources: Rio Paraná Energia S.A. (ANEEL PD-10381-0322/2022), CNPq (Carlos Kebudi, project 130236/2021-7, and Bruno Fânzeres, project 309064/2021-0), FAPERJ (Bruno Fânzeres, project E-26/202.825/2019), and CTG Brazil Group (ANEEL PD-10381-0322/2022).
- Everyone who inspired and influenced me during my academic journey.

Abstract

Orlando, Carlos Alberto Kebudi; Santos, Bruno Fânzeres (Advisor). **Optimal Wind Farm Layout Design Accounting for Wake Effects and Contracting Strategies**. Rio de Janeiro, 2023. 56p. Dissertação de Mestrado – Departamento de Engenharia Industrial, Pontifícia Universidade Católica do Rio de Janeiro.

As the world confronts the pressing issue of climate change, wind power stands out as a critical source of clean energy. However, realizing its full potential relies on the optimization of wind farm layouts, particularly in light of the complex wake effect. This dissertation delves into Wind Farm Layout Optimization (WFLO) using the Bastankhah Wake Model. The scope of this study goes beyond layout design; it encompasses the intricate task of mitigating the wake effect's impact along with the seek for a risk-averse-value maximizing trading strategy. To account for risk-averseness, a combination between Expected Value and the left-side-quantile-based risk-measure functionals, the Conditional Value-at-Risk (CVaR) measure. To support this research, an open-source package `OptimalLayout.jl` was developed. This package co-optimizes the positioning of wind turbines to mitigate wake effect impact, and the contracting strategy of a Risk-Averse agent/generator. Through a series of practical case studies across diverse dynamic environments, this research illustrates the real-world applicability of WFLO. These investigations intricately examine its influence on power production and revenue dynamics, offering valuable insights into sustainable energy solutions.

Keywords

Wind Farm Layout Optimization; Bastankhah Wake Model; Conditional Value at Risk; Energy Economics; Contracting Strategies; Wake Effect.

Resumo

Orlando, Carlos Alberto Kebudi; Santos, Bruno Fânzeres. **Desenho Parque Eólico Considerando Wake Effects e Estratégias de Contratação**. Rio de Janeiro, 2023. 56p. Dissertação de Mestrado – Departamento de Engenharia Industrial, Pontifícia Universidade Católica do Rio de Janeiro.

À medida que o mundo enfrenta a urgente questão das mudanças climáticas, a energia eólica se destaca como uma fonte crítica de energia limpa. No entanto, realizar seu pleno potencial depende da otimização dos layouts de parques eólicos, especialmente à luz do complexo efeito de esteira. Esta dissertação adentra na Otimização de Layout de Parques Eólicos (WFLO, na sigla em inglês) usando o Modelo de Efeito de Esteira de Bastankhah. O escopo deste estudo vai além do design de layout; abrange a intrincada tarefa de mitigar o impacto do efeito de esteira, juntamente com a busca por uma estratégia de negociação com aversão ao risco e maximização de valor. Para contabilizar a aversão ao risco, uma combinação entre o Valor Esperado e os funcionais de medida de risco baseados no quantil esquerdo, a medida de Valor em Risco Condicional (CVaR). Para apoiar esta pesquisa, um pacote de código aberto `OptimalLayout.jl` foi desenvolvido. Este pacote co-otimiza o posicionamento das turbinas eólicas para mitigar o impacto do efeito de esteira e a estratégia de contratação de um agente/gerador avesso ao risco. Através de uma série de estudos de casos práticos em diversos ambientes dinâmicos, esta pesquisa ilustra a aplicabilidade do WFLO no mundo real. Estas investigações examinam detalhadamente a sua influência na produção de energia e na dinâmica das receitas, oferecendo informações valiosas sobre soluções energéticas sustentáveis.

Palavras-chave

Otimização de Parque Eólico; Bastankhah Wake Model; Conditional Value at Risk; Economia da Energia; Estratégias de Contrato; Efeito Esteira.

Table of contents

1	Introduction	11
2	Modeling Bastankhah's wake effect	15
2.1	Evolution of Bastankhah's Wake Effect Modeling	15
2.2	Yaw Angle Influence	17
2.3	Production-Only Wind Farm Optimization	17
3	WFLO Model With Wake Effect and Contracting Strategy	19
3.1	Wind Farm Cash Flow	19
3.2	Risk Profile Representation (CVaR)	20
3.3	Optimization Model	20
4	OptimalLayout.jl: Modeling and Solving Wind Farm Layout Design Accounting for Wake Effects and Contracting Strategies	22
5	Case Study	26
5.1	Experimental Setup	26
5.2	Illustrative example	27
5.3	Case setup description	27
5.4	Layout Optimization: Case Study	30
5.5	Experimental analysis and results	32
5.6	Baseline Analysis	32
5.7	Sensitivity Analysis	45
5.8	Analysis over current practices	49
6	Conclusions	52
7	References	53

List of figures

Figure 2.1	Wind in a Gaussian Distribution after passing through the rotor	16
Figure 4.1	Chart of FLOWFarm.jl, SNOW.jl, and OptimalLayout.jl after optimization.	23
Figure 5.1	Illustration of the wind speed, with $\alpha = 2.5$. Vertical axis means the height and horizontal means lateral distance.	28
Figure 5.2	Illustration of the wind speed, with $\alpha = 4.0$. Vertical axis means the height and horizontal means lateral distance.	28
Figure 5.3	Illustration of the wind speed, with $\alpha = 5$. Vertical axis means the height and horizontal means lateral distance.	29
Figure 5.4	Wind farm scheme	29
Figure 5.5	Wind Speed in Rio Grande do Norte, in the year of 2020	31
Figure 5.6	(Left) Baseline Case: An evenly spaced wind farm layout; (Right) Optimal layout changes the position of the turbines, in order to produce more energy.	31
Figure 5.7	Energy prices in the Northeast of Brazil (2010 - 2020)	32
Figure 5.8	Wind Speed and Direction in Northeast, in years of 2010 - 2020	33
Figure 5.9	Baseline Analysis - Evenly Spaced	34
Figure 5.10	Baseline Analysis - Real Case	34
Figure 5.11	Baseline Analysis - Optimized	35
Figure 5.12	Violin Plot Distribution - Evenly Spaced	36
Figure 5.13	Violin Plot Distribution - Real Case	37
Figure 5.14	Power Production: Evenly Spaced vs Optimized	38
Figure 5.15	Power Production: Real Case vs Optimized	38
Figure 5.16	Power Production: Evenly Spaced vs Optimized - Range I	39
Figure 5.17	Power Production: Evenly Spaced vs Optimized - Range II	39
Figure 5.18	Power Production: Evenly Spaced vs Optimized - Range III	40
Figure 5.19	Power Production: Real Case vs Optimized - Range I	40
Figure 5.20	Power Production: Real Case vs Optimized - Range II	41
Figure 5.21	Power Production: Real Case vs Optimized - Range III	41
Figure 5.22	Power Production Comparison: Evenly Spaced vs Optimized	42
Figure 5.23	Power Production Comparison: Real Case vs Optimized	42
Figure 5.24	Power Production Comparison: Evenly Spaced vs Optimized - Spring.	43
Figure 5.25	Power Production Comparison: Evenly Spaced vs Optimized - Winter.	43
Figure 5.26	Power Production Comparison: Evenly Spaced vs Optimized - Autumn.	43
Figure 5.27	Power Production Comparison: Real Case vs Optimized - Spring.	44
Figure 5.28	Power Production Comparison: Real Case vs Optimized - Winter.	44
Figure 5.29	Power Production Comparison: Real Case vs Optimized - Autumn.	44

Figure 5.30	Power Production Comparison: Evenly Spaced vs Optimized - Summer.	45
Figure 5.31	Power Production Comparison: Real Case vs Optimized - Summer.	45
Figure 5.32	Contract Variation - Total Average Revenue: Real Case vs Optimized.	46
Figure 5.33	Contract Variation - CVaR: Real Case vs Optimized.	47
Figure 5.34	Contract Variation - %FEC: Real Case vs Optimized.	47
Figure 5.35	λ Variation - Total Average Revenue: Real Case vs Optimized.	48
Figure 5.36	λ Variation - CVaR: Real Case vs Optimized.	48
Figure 5.37	λ Variation - %FEC: Real Case vs Optimized.	49
Figure 5.38	Sequential Layout with contract cost = R\$240.00 and $\lambda = 0.4$.	50
Figure 5.39	Optimal Layout with contract cost = R\$240.00 and $\lambda = 0.4$.	50

List of tables

Table 5.1	Wind farm parameters	26
Table 5.2	Wind farm parameters	27
Table 5.3	Wake Effect Results (ΔU)	29
Table 5.4	AEP Comparison	32
Table 5.5	Layout Performance Comparison	35
Table 5.6	Monthly Average Revenue Table	35
Table 5.7	Layout Performance Comparison	50
Table 5.8	Average Revenue Comparison	51

1

Introduction

The urgency to combat climate change and transition to a low-carbon energy future has never been more critical. Recent reports from the Intergovernmental Panel on Climate Change (IPCC) underscore the urgency of limiting global warming to just 1.5 degrees Celsius above pre-industrial levels to avert catastrophic consequences [1]. However, despite growing awareness, global greenhouse gas emissions continue to rise, driven by the enduring dominance of carbon-intensive industries [2]. Given the substantial role of the energy sector in emissions, there is an escalating need to expedite the adoption of renewable energy sources. Among these, wind power shines as a promising avenue for delivering clean and sustainable electricity.

In recent years, the wind energy sector has witnessed remarkable growth, with wind farms becoming integral to the global energy landscape [3]. In the specific context of Brazil, a country with vast wind energy potential, understanding and harnessing these resources efficiently are of utmost importance. Research by the International Renewable Energy Agency (IRENA) has emphasized Brazil's substantial wind power potential and its capacity to harness wind resources for clean electricity generation [4]. Such knowledge is instrumental in optimizing wind farm performance and contributing to Brazil's aspirations of increasing the share of renewables in its energy mix.

The variable nature of wind resources, dictated by fluctuations in wind speed and direction over time [5, 6], presents a formidable challenge to maximizing the benefits of wind power [7]. Tackling this challenge necessitates innovative solutions in Wind Farm Layout Optimization (WFLO) [8, 9], taking into account both technical [10] and economic considerations [11]. Additionally, optimizing the spatial arrangement of wind turbines can mitigate wake losses [12, 13] and augment power output in wind farms [14]. These research endeavors make substantial contributions to global knowledge on wind farm optimization, playing a pivotal role in shaping sustainable wind energy projects in the country.

Furthermore, beyond the physical layout of wind farms, the intricacies of energy trading and pricing within electricity markets have undergone significant changes over the years. This transformation became especially pronounced when hourly energy spot prices were introduced in Brazil, leading to increased price volatility [15, 16, 17]. Consequently, when observed from the perspective of a Wind Energy Producer, engaging in bilateral contracts

that guarantee the delivery of a fixed energy quantity exposes the producer to the well-recognized risks associated with price and quantity fluctuations [18, 19]. These variability are attributed to the seasonality and intermittent nature inherent in wind patterns [20]. Additionally, recent research has been dedicated to the development of risk-constrained optimal trading strategies [21, 22, 23]. This approach offers valuable insights into risk management and the optimization of decisions in dynamic electricity markets [24, 25].

In this context, the study explores WFLO and strategies for addressing energy trading and pricing challenges in Brazil. To represent the Wake Effect modelling, it will be used the Bastankhah method [26]. This method enhances the standard ones, such as the Jensen method [27], by accounting for a Gaussian-like wake losses, yaw angle of the turbine and wake width. On the other hand, an optimal contracting strategy framework is also accounted by based on two-stage risk-averse decision process. More specifically, it was considered a long-term Forward Contract to back the wind farm project financing similar to a Power Purchase Agreement (PPA) with a consumer. To identify the optimal involvement in this Forward Contract, a combination between Expected Value and the left-side-quantile-based risk-measure functional, the Conditional Value-at-Risk (CVaR) is used to formulate the model that devises the optimal contract strategy. Finally, to support this research, an open- source package¹ was developed. Furthermore, it was used `FLOWFarm.jl` library and `SNOW.jl` (Sparse Nonlinear Optimization Wrapper) in order to build the machinery to calculate the wind power production for a given turbine positioning and wind farm and flow parameters. On of these packages, we construct the decision-support tool `OptimalLayout.jl` that seeks for the optimal location of the turbines and the amount of Forward Contract involvement that maximizes the wind farm risk-adjusted long-term net revenue.

Three case studies of a wind farm in Northeast Brazil assess the impact of layout optimization on power production. First, an in-depth analysis of the annual energy generation achieved by an optimized model is presented. The second case involves a revenue comparison using a benchmark model, where turbine coordinates and contracts are optimized, and the sensitivity of contract pricing and risk regulation parameters is analyzed. Lastly, the co-optimized instance is contrasted with the process of sequential optimization for a comprehensive assessment.

Thus, the contributions of this study are as follows:

1. **Framework Proposal:** A novel framework for wind farm layout design is introduced, incorporating considerations of the wake effect and con-

¹Available at: <https://github.com/ckebugdi/OptimalLayout>.

tracting. This framework not only addresses the technical aspects, such as the Bastankhah Wake Model but also delves into the Commercial aspect, involving the identification of a risk-averse long-term strategy for financing the park’s construction;

2. **Package Tool Development:** An efficient package tool implemented in Julia is provided. This tool extends wind simulation capabilities, utilizing an open source package in order to optimize energy generation throughout the year. This extension enables the formulation and solution of the optimization problem related to agent revenue;
3. **Real-World Application:** The framework’s practical applicability is demonstrated through a real case study in Northeast of Brazil. By comparing the performance of an optimized layout with an evenly spaced and real wind farm layouts, valuable insights into revenue, generation and risk metrics for energy agents are obtained. Additionally, a comparison between the sequential optimization approach and the co-optimization process is presented, revealing performance findings.

To better understand the structure of this work, the subsequent sections of the dissertation are organized as follows: Section 2 introduces Bastankhah’s Wake Effect model along with the integration of yaw angles in Section 2.2. Section 3 delves into contractual considerations and the formulation of the revenue equation. Furthermore, it introduces the integration of risk measures into the optimization problem and showcases the co-optimization between contracts and turbine layouts. Section 4 provides a detailed overview of the sequence of steps in the Optimization Problem, starting from the initial setup and progressing through each stage of the optimization process, while also explaining the roles of each employed package. Subsequently, Section 5 presents the results of the case studies and their optimization outcomes, while Section 6 offers the final conclusions.

The scientific and technological products related to this dissertation are:

1. Carlos Kebudi and Bruno Fanzeres, “Optimal Wind Farm Layout with Bastankhah Model,” in *Proc. 2023 IEEE Power & Energy Society General Meeting (PESGM)*, July 2023. DOI: 10.1109/PESGM52003.2023.10252938
2. Carlos Kebudi, Andrew Rosemberg, and Bruno Fanzeres, “Optimal Wind Farm Layout Design Accounting for Wake Effects and Contracting Strategies,” *to be submitted to Applied Energy*.

3. *Open-Source Package* OptimalLayout.jl – Available at: <https://github.com/ckebugdi/OptimalLayout>

2

Modeling Bastankhah's wake effect

The modeling section is twofold: Firstly, the Bastankhah wake model will be developed up to its simplified form [26]. Secondly, subsequent enhancements to the model are discussed in Section 2.2, where the influence of turbine yaw angles on wake effects is explored [28]. Additionally, the section outlines the methodology for computing the Annual Energy Production (AEP) using wake models [29].

2.1

Evolution of Bastankhah's Wake Effect Modeling

The initial stage in establishing the wind farm's wake analysis involves the incorporation of mass and momentum equations while neglecting viscous and pressure terms, in line with Tennekes' insights [30]:

$$T = \phi \int U_w (U_\infty - U_w) dA \quad (2-1)$$

Here, T signifies the total force exerted on the turbine, ϕ represents the air density, and U_w stands for the wind velocity behind the turbine. Burton [31], provides a means to determine T as follows:

$$T = \frac{1}{2C_T \phi A_0 U_w^2} \quad (2-2)$$

In this equation, C_T is the Coefficient of Thrust and A_0 signifies the swept area covered by the wind turbine blades. For the present study, the initial focus is on elucidating the velocity deficit within the turbine wake. This can be achieved by introducing the velocity deficit $C(x)$, defined as:

$$\frac{\Delta U}{U_\infty} = C(x) \cdot f\left(\frac{r}{\zeta(x)}\right) \quad (2-3)$$

Here, $C(x)$ characterizes the normalized velocity deficit at each down-wind position, aligned with the wake's center. The function f encapsulates the reduction factor associated with an exponential distribution, while $\zeta(x)$ represents the wake's characteristic width at a given x , and r denotes the radial distance from the wake's center. Given the Gaussian nature of the velocity deficit within the turbine wake, the equation is reformulated as:

$$\frac{\Delta U}{U_\infty} = C(x) e^{-\frac{r^2}{2\sigma^2}} \quad (2-4)$$

The rearranged equations allow for the expression of wake-normalized velocity as:

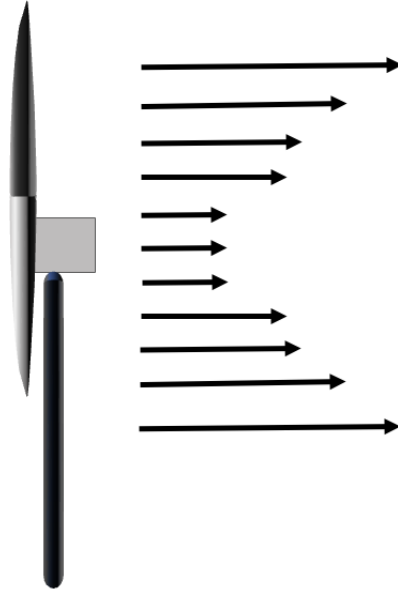


Figure 2.1: Wind in a Gaussian Distribution after passing through the rotor

$$U_w = U_\infty \left(1 - C(x) e^{-\frac{r^2}{2\sigma^2}} \right) \quad (2-5)$$

In 2-5, σ denotes the standard deviation of the Gaussian-like velocity deficit profiles at each x . The subsequent step involves combining equations (2-2) and (2-5), inserting them into the mass and momentum conservation equation (2-1), and then integrating the equation from 0 to ∞ . Upon solving, two values are obtained, but only one of them accurately predicts the smaller velocity deficit at greater downwind distances:

$$C(x) = 1 - \sqrt{\frac{1 - C_t}{8 \left(\frac{\sigma}{d_0} \right)^2}} \quad (2-6)$$

Moreover, Jensen's work [27] suggests a linear expansion for the wake region's σ/d_0 ratio, expressed as:

$$\frac{\sigma}{d_0} = \frac{kx}{d_0} + \epsilon \quad (2-7)$$

In this equation, $k = \partial\sigma/\partial x$ represents the growth rate, and ϵ approximates the value of σ/d_0 as x approaches zero. Incorporating (2-6) and (2-7) into (2-4), followed by rearranging, leads to the final expression:

$$\frac{\Delta U}{U_\infty} = \left(1 - \sqrt{1 - \frac{C_t}{8 \left(\frac{kx}{d_0 + \epsilon} \right)^2}} \right) e^{-0.5 \left(\frac{z - z_h}{d_0} \right)^2} e^{-0.5 \left(\frac{y}{d_0} \right)^2} \quad (2-8)$$

In this equation, y and z represent the spanwise and vertical coordinates, while z_h pertains to the hub height. This equation captures the normalized velocity deficit within the wake, expressed as a function of normalized coordinates (x/d_0 , y/d_0 , and z/d_0 , C_T , and k).

It's worth noting that Baker [32] refers to the model that omits consideration of wind angles as the "Simplified Bastankhah" model. To employ equations dependent on ϵ , its value must be pre-determined. This can be accomplished by substituting $x = 0$ into the total mass flow deficit rate, as formulated in the Frandsen model [33]. Thus, ϵ is given by:

$$\epsilon = 0.25\sqrt{\beta} \quad (2-9)$$

2.2

Yaw Angle Influence

This subsection delves into the impact of turbine yaw angles on wake effects. This model assumes yawed turbines to mitigate wake interactions resulting from wind direction changes. The motivation for this perspective stems from the potential to enhance energy production within wind farms, as highlighted in the works of Jimenez [34] and Bastankhah [35].

$$\frac{\Delta U}{U_\infty} = \left(1 - \sqrt{1 - \frac{C_t \cos \gamma}{8(\sigma_y \sigma_z / d^2)}}\right) e^{-0.5\left(\frac{y-\zeta}{\sigma_y}\right)^2} e^{-0.5\left(\frac{z-z_h}{\sigma_z}\right)^2} \quad (2-10)$$

In this equation, σ symbolizes the characteristic wake width, and it's deduced that σ_y and σ_z denote the wake's widths in the lateral (y) and vertical (z) directions, respectively. Consequently, to ascertain σ_y and σ_z :

$$\frac{\sigma_y}{d} = k_y \frac{x}{d} + \frac{\cos \gamma}{\sqrt{8}} \quad (2-11)$$

$$\frac{\sigma_z}{d} = k_z \frac{x}{d} + \frac{1}{\sqrt{8}} \quad (2-12)$$

2.3

Production-Only Wind Farm Optimization

Efficiently expanding wind power's presence in the global energy generation mix poses a significant challenge. The goal is to strategically position turbines within confined spaces to optimize wind farm production, considering various physical factors, notably the wake effect. To address this challenge, the Bastankhah Wake Model, detailed in Section 2.1, is leveraged to formulate the WFLO problem:

$$\max_{(\mathbf{x}, \mathbf{y}) \in \Xi} \left\{ \sum_{l=1}^n g_l(\mathbf{x}, \mathbf{y}, U_w) \right\} \quad (2-13)$$

In this equation, Ξ represents the physical region available for wind turbine placement, and g_l is a function assessing the power generated by wind turbine $l \in \{1, \dots, n\}$ based on a specific farm layout (\mathbf{x}, \mathbf{y}) .

3

WFLO Model With Wake Effect and Contracting Strategy

This section delves into the modeling of contract types, followed by the representation of risk profiles in the energy sector. The commercialization of energy involves various aspects of risk and contract management, making it crucial for market participants to employ robust models and risk measures.

3.1

Wind Farm Cash Flow

In the Brazilian energy market, a pivotal risk management tool is the financial forward contract, locally referred to as the "contract by quantity." This contract structure places the responsibility for energy delivery squarely with the producer. Interestingly, the producer isn't obliged to physically generate the exact contracted quantity; instead, they are required to settle any discrepancy between the actual and contracted energy volumes in the spot market. Consequently, the spot market serves as a clearing platform where negotiations for energy shortfalls and surpluses take place, all at prevailing spot prices as can be seen in (3-1). It's worth noting that these contracts are invaluable instruments for safeguarding against fluctuations in spot prices.

The revenue for a generation company (Genco) or an Energy Trading Company (ETC), when selling electricity (avgMW) in a financial forward contract at a price (P) denominated in R\$/MWh, quantity (Q) and hours in a specific time can be calculated using the following expression (assuming production costs are not taken into account):

$$f^{(F)} = P Q h_t + \left(\tilde{g}(x, y, U_w) - Q h_t \right) \tilde{\pi}. \quad (3-1)$$

Transitioning from Equation 3-1 to Equation 3-2, the focus shifts to an agent's revenue flow over time through a forward contract. The latter equation provides a detailed insight into how revenue accumulates for a Genco or an ETC as they operate over multiple time periods:

$$R_a \left(Q, g(\mathbf{x}, \mathbf{y}, \tilde{U}_w), \tilde{\pi} \right) = \sum_{t \in \mathcal{H}_a} \left(P Q h_t + \left(g(\mathbf{x}, \mathbf{y}, \tilde{U}_w) - Q h_t \right) \tilde{\pi}_t \right). \quad (3-2)$$

Where \mathcal{H}_a is the set of hours in an year $a \in \mathcal{A}$.

3.2

Risk Profile Representation (CVaR)

The energy sector is primarily composed of risk-averse entities. Consequently, this analysis employs the Conditional Value-at-Risk (CVaR) as the chosen risk metric. The CVaR measures the average magnitude of potential losses faced by an entity within a given portfolio, providing insights into the distribution of extreme outcomes. Let $(\Omega, \mathcal{F}, \mathbb{P})$ represent a probability space with a discrete sample space Ω (comprising various scenarios). Within this context, the revenue's random variable in Equation (3-2) can be characterized as depicted in Equation (3-3).

$$\tilde{R} = \{R_\omega, p_\omega\}_{\omega \in \Omega}. \quad (3-3)$$

The CVaR of the revenue distribution in Equation (3-3) can be calculated using the mathematical programming problem defined in the equation below:

$$CVaR_\alpha(\tilde{R}) = \max_{z, \delta_\omega} z - \frac{1}{1 - \alpha} \sum_{\omega \in \Omega} p_\omega \delta_\omega \quad (3-4)$$

subject to:

$$\delta_\omega \geq z - R_\omega, \quad \forall \omega \in \Omega; \quad (3-5)$$

$$\delta_\omega \geq 0, \quad \forall \omega \in \Omega. \quad (3-6)$$

In (3-4)–(3-6), α represents the significance level chosen by the decision-maker to measure the "size" of the tail of losses in the revenue distribution. z is the Value at Risk (VaR), and δ_ω is an auxiliary variable used for calculating the Conditional Value-at-Risk (CVaR). In this formulation, it is identified the average of the $(1 - \alpha)$ worst-case scenarios in the revenue distribution. Furthermore, the constraints in (3-5) pertain to the difference between VaR and revenue for each scenario, with the requirement that this term should be greater than or equal to zero as specified in (3-6) [36].

3.3

Optimization Model

In this section, the contracting and positioning coordinates problem are merged. In a broad sense, the decision-making framework aims to maximize the CVaR for contractual and operational cash flows by identifying the optimal allocation of contracts. The following optimization model structure is under study:

$$\begin{aligned} \max_{\mathbf{x}, \mathbf{y}, Q} \lambda \text{CVaR}_\alpha \left(\left\{ R_a \left(Q, g(\mathbf{x}, \mathbf{y}, \tilde{\mathbf{U}}_w), \tilde{\boldsymbol{\pi}} \right) \right\}_{a \in \mathcal{A}} \right) \\ + (1 - \lambda) \sum_{a \in \mathcal{A}} \left(\mathbb{E} \left[R_a \left(Q, g(\mathbf{x}, \mathbf{y}, \tilde{\mathbf{U}}_w), \tilde{\boldsymbol{\pi}} \right) \right] \right) \end{aligned} \quad (3-7)$$

subject to:

$$(\mathbf{x}, \mathbf{y}) \in \Xi \quad (3-8)$$

$$0 \leq Q \leq \bar{Q} \quad (3-9)$$

The optimization model (3-7)–(3-9) is designed to maximize the agent's expected earnings while considering associated risks measured by the CVaR of the yearly revenue. The decision variables encompass Quantity contracts (Q) and the spatial coordinates of the wind farm (\mathbf{x} and \mathbf{y}). Constraint (3-8) ensures that the wind turbine coordinates, represented by \mathbf{x} and \mathbf{y} , remain within the designated wind farm area denoted as Ξ . Lastly, (3-9) stipulates that the contract quantity (Q) must fall within the range of 0 and the Physical Guarantee (\bar{Q}) of the park. In (3-7), $\lambda \in [0, 1]$ outlines the general risk-aversion level embedded within the wind farm investor. More specifically, $\lambda = 0$ induces a risk-neutral agent and, as $\lambda \rightarrow 1$, the CVaR component is highlighted, leading to a more risk-averse decision-making process. It should be noted that the optimization model (3-7)–(3-9) lies within the class of non-convex programming problems, thus challenging to be solved using standard optimization algorithms or off-the-shelf solvers. In the next chapter, we present a package named `OptimalLayout.jl` constructed to efficiently handle and manipulate this decision problem.

OptimalLayout.jl: Modeling and Solving Wind Farm Layout Design Accounting for Wake Effects and Contracting Strategies

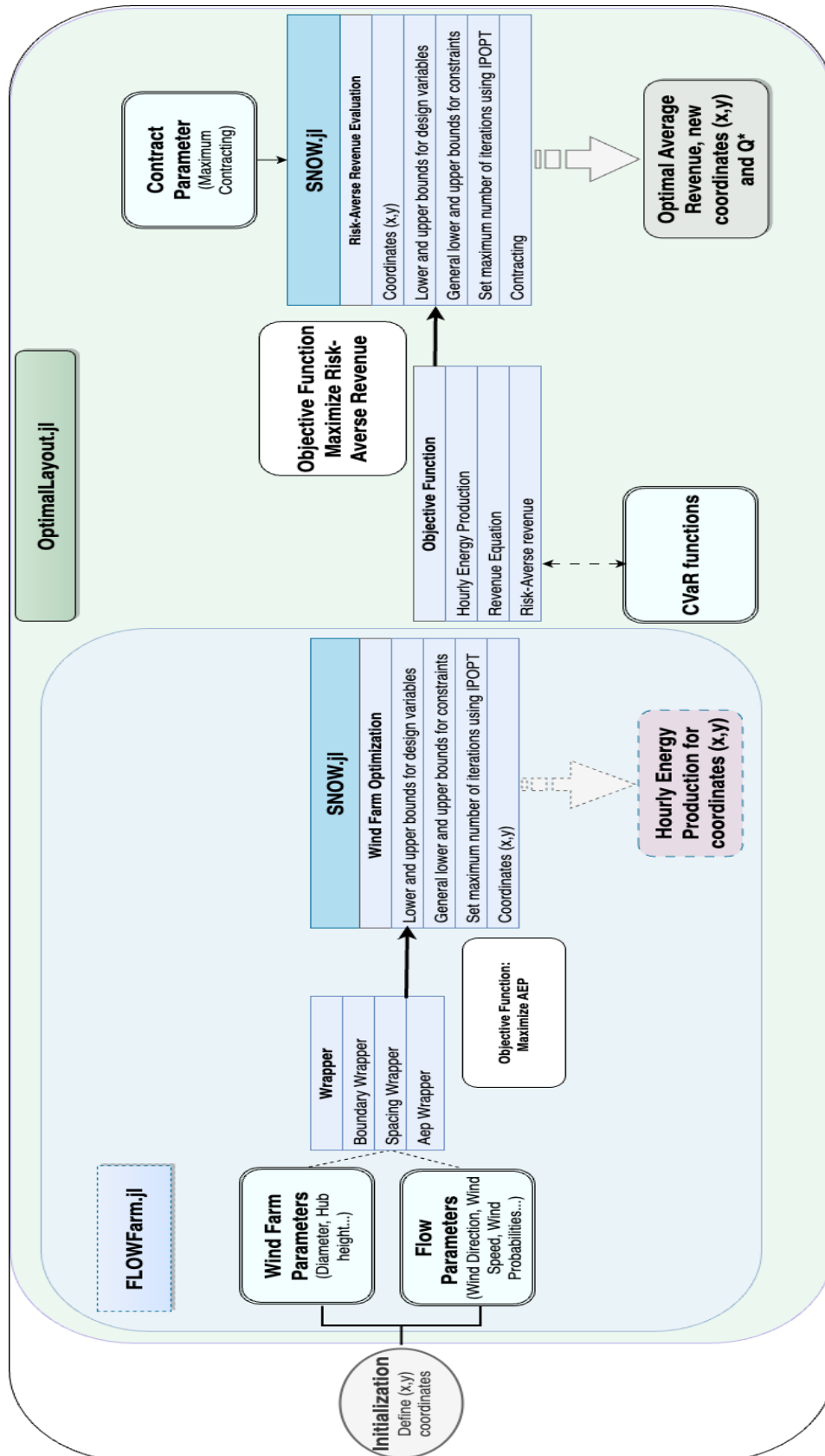


Figure 4.1: Chart of FLOWFarm.jl, SNOW.jl, and OptimalLayout.jl after optimization.

In this chapter, a visual representation (4.1) outlines the sequential steps involved in optimizing Wind Farm Layouts, Revenue, and Contracting. This visual diagram serves as an illustrative guide, elucidating the input parameters, the utilization of the `FLOWFarm.jl` library, its integration with the SNOW (Sparse Nonlinear Optimization Wrapper) framework, and the new package, `OptimalLayout.jl`, which includes Contract Optimization, and consequently, Revenue optimization.

FLOWFarm.jl: This package is a Julia-based computational library meticulously designed for the optimization of wind farm layouts. It equips users with essential tools to strategically place wind turbines within predefined areas. The primary objective is to maximize energy production while carefully considering site-specific constraints and objectives. Salient features of `FLOWFarm.jl` include advanced turbine wake modeling, wind flow simulation, optimization capabilities, and seamless integration with external optimization solvers. Additionally, the library offers boundary control functions to ensure harmonious turbine placement within predefined geographic boundaries.

SNOW.jl: The integration with SNOW plays a pivotal role in streamlining the optimization process. Serving as an indispensable bridge, it seamlessly connects the `FLOWFarm` library with potent external nonlinear optimization solvers, including IPOPT. This integration enables the effective translation of the complex optimization problem formulated within the `FLOWFarm` framework into a format that can be efficiently processed by these solvers.

OptimalLayout.jl: Finally, this package is introduced as a purpose-built package crafted to optimize wind farm layout and agent contracts. This pioneering approach strives to maximize the revenue generated by a risk-averse agent while concurrently refining the turbine layout within the wind farm. By adeptly addressing both layout design and contract negotiation, `OptimalLayout.jl` confronts the critical challenges pertaining to financial viability and risk management prevalent within the wind energy sector.

Flowchart: Regarding the flowchart, a step-by-step representation will be shown to represent the flow until the optimization. Here are as follows:

I - Initialization - Setting \mathbf{x} and \mathbf{y} coordinates: Define the coordinates for wind turbines in the wind farm layout, representing their physical locations within the designated area.

II - Wind Farm Parameters and Flow Parameters: Configure wind farm parameters and flow parameters to establish essential settings for wind farm

modeling and simulation. Example: Wind turbine specifications are specified as part of wind farm parameters. Flow parameters define how the wind flows through the landscape and how turbines interact with each other.

III - Wrapper Functions: These functions serve as intermediaries between the user-defined wind farm model and the optimization solver. They encapsulate the optimization problem, making it amenable to solution by external solvers.

IV - `SNOW.jl` (Sparse Nonlinear Optimization Wrapper): This is a critical component in the optimization process. It involves several aspects:

- i - Define lower and upper bounds for design variables;
- ii - Specify general lower and upper bounds for constraints;
- iii - Set a maximum number of iterations using IPOPT;
- iv - Utilize coordinates (\mathbf{x}, \mathbf{y}) as design variables;
- v - Contracting (used just in the `OptimalLayout.jl` package): Define the maximum allocation of the contract concerning the physical guarantee of the wind park.

If the final objective is Revenue Optimization, consider the `OptimalLayout.jl`, where the objective function extends beyond AEP maximization. It incorporates additional components (Equations (3-7), (3-8), and (3-9)) to introduce CVaR functions, identifying the average of the worst-case scenarios in the revenue distribution.

V - Optimization: The final step in the flowchart is the optimization process itself. With all parameters, constraints, and bounds defined, the optimization solver is invoked to find the optimal wind farm layout that maximizes the specified objective function.

5 Case Study

This section presents three numerical cases, demonstrating how optimized layouts influence on energy generation, contracting and revenue, within the context of a wind farm located in Northeast Brazil. In the first example, the impact of turbine positioning optimization on energy production is examined. The second scenario introduces the Contracting Model into the optimization problem and assesses its effects on the agent's Revenue and CVaR. The third instance provides a comparative analysis, contrasting the outcomes of a co-optimized Model with those of a sequential optimization approach, revealing notable distinctions.

5.1 Experimental Setup

In this subsection, the parameters for the case setup and case studies 5.4 and 5.5 are presented. Table 5.1 outlines the default values of a Julia package, which were used in the initial case study (5.4) as well as the Case Setup Description (5.2). The next set of parameters (Table 5.5) provides a detailed analysis to case 5.5 of the values associated with a Vestas V82 turbine. These values include the rotor diameter (d_0), Cut-in speed (C_{in}), Cut-out speed (C_{out}), Rated Speed (R_s), Rated Power (R_p), and relevant wind farm physical characteristics, such as circle radius (R_{ad}) and minimum turbine-to-turbine distance ($dist_{min}$). The wind direction and speed data for Subsection 5.4 pertains to the year 2020, while subsequent sections (5.5) rely on data spanning the years 2010-2020."

Table 5.1: Wind farm parameters

Parameters		
d_0	80	meters
Z_h	70	meters
U_∞	10	m/s
C_t	0.8	-
ϕ	1.1716	kg/m^3
\mathbf{k}	0.075	-
ϵ	$1/\sqrt{8}$	-
R_{ad}	400.0	meters
$dist_{min}$	160.0	meters

Table 5.2: Wind farm parameters

Parameter	Value	Unit
d_0	82	meters
Z_h	60	meters
C_{in}	3.5	m/s
C_{out}	20.0	m/s
R_s	13.0	m/s
R_p	1.65e6	Watts
C_t	0.8	-
ϕ	1.1716	kg/m ³
k	0.075	-
ϵ	1/ $\sqrt{8}$	-
R_{ad}	1087.92	meters
dist _{min}	160.0	meters

5.2

Illustrative example

An illustrative numerical example is presented to expose the consequences of the wake effect and the yaw angle of the turbines. The idea is to simulate a case of a wind farm with two turbines, with the following case setup:

5.3

Case setup description

Three wake effects will be shown in the figures 5.1, 5.2, 5.3. This experiment uses the following types of axis: x , y and z . In this case, the variable that will vary is x/d_0 (which it will be called α) in three different ways: near wake x/d_0 ($\alpha = 2.5$), medium wake x/d_0 ($\alpha = 4.0$) and far wake x/d_0 ($\alpha = 5$). It is possible to notice that the higher the α , the less is the impact of the wake effect in the second turbine. Visibly, it is noticed that the blur disappears as the values of y and z increase.

Moving forward, figure 5.4 explains the wind farm scheme. When the free wind (w_∞) reaches the rotor turbine, not necessarily it will reach aligned to the rotor. So, there's an angle of impact in the rotor turbine, and this is why it is necessary to consider the cosine of the angle in the turbine. In this first case, it is considered the most simplistic case, with the wind aligned to the rotor. In the next experiment, the wind direction will be considered.

Figure 5.4 shows that not only the velocity of the wind and the yaw angle of turbine impacts in the final result of the power production, but also the layout of a wind farm. The way of the positioning the wind turbines are circumstantial to reach the best layout of contract.

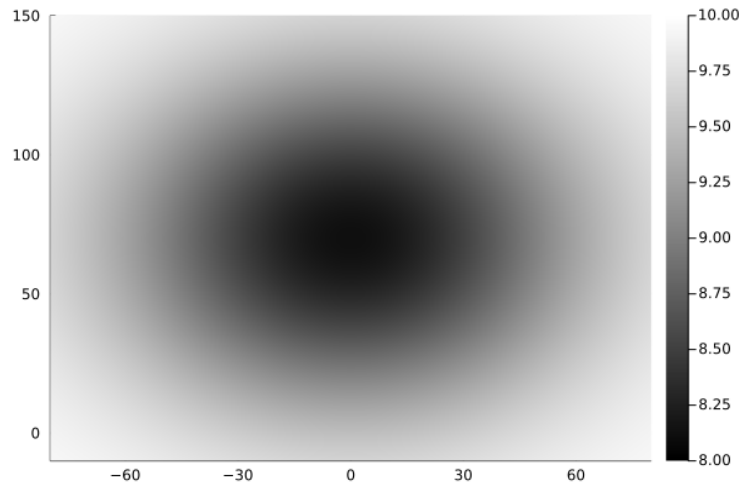


Figure 5.1: Illustration of the wind speed, with $\alpha = 2.5$. Vertical axis means the height and horizontal means lateral distance.

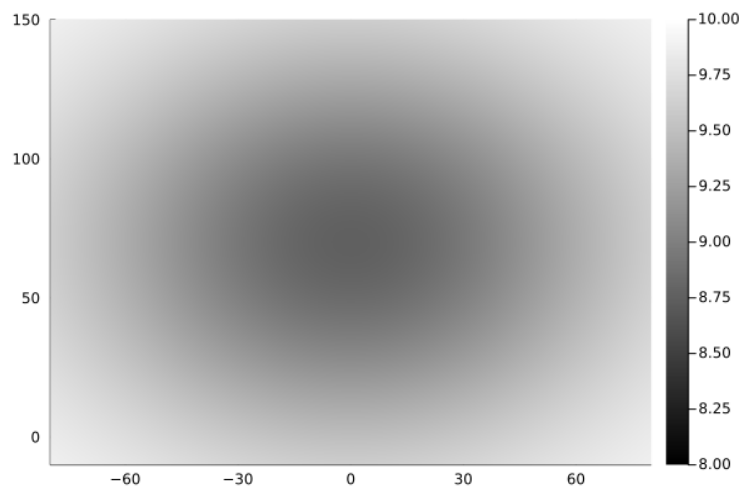


Figure 5.2: Illustration of the wind speed, with $\alpha = 4.0$. Vertical axis means the height and horizontal means lateral distance.

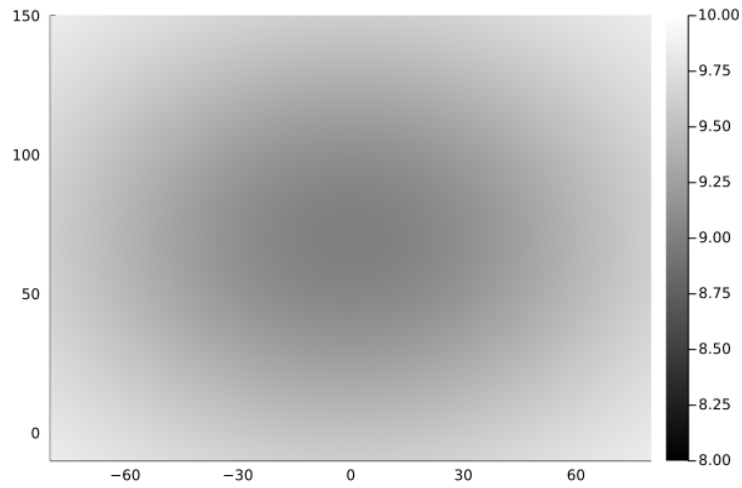


Figure 5.3: Illustration of the wind speed, with $\alpha = 5$. Vertical axis means the height and horizontal means lateral distance.

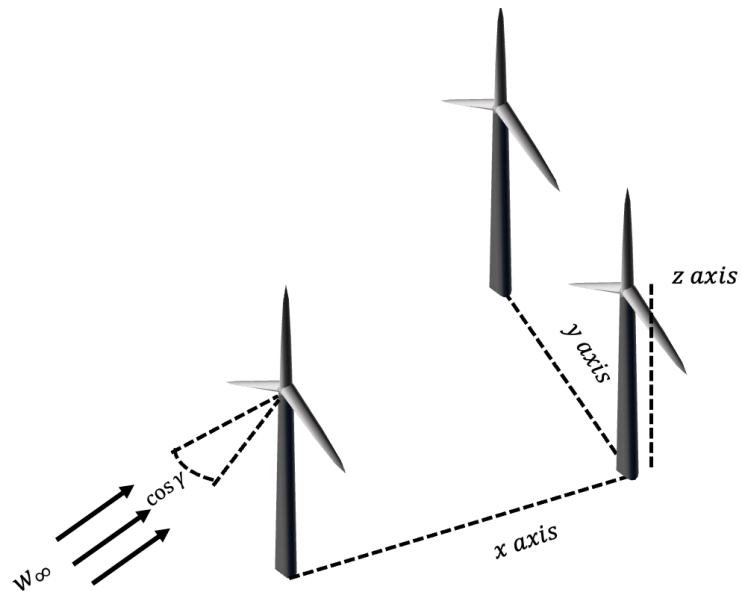


Figure 5.4: Wind farm scheme

Table 5.3: Wake Effect Results (ΔU)

$\alpha \backslash \gamma$	0	15	50	75	100
2	82.49%	83.41%	90.39%	95.51%	98.48%
5	91.17%	91.43%	93.63%	95.77%	97.62%
10	96.01%	96.07%	96.58%	97.17%	97.83%
15	97.75%	97.77%	97.94%	98.15%	98.41%
20	98.56%	98.57%	98.64%	98.73%	98.85%

The analysis of Table 5.3, regards the possibility of the impact from the wake effect in the turbines (assuming $\gamma = 0$), since this table represents $\Delta U = \frac{U_\infty - U_w}{U_\infty}$. The horizontal axis $y_0 = \{0,15,50,75,100\}$ and the vertical axis $x/d_0 = \{2,5,10,15,20\}$ represents the distances between turbines. In other words, the closer the values are to 100%, the smaller the wake effect. Therefore, when x/d and y values are high, it means that the turbines are far from each other. The lower value of y axis and x/d (0 and 2, respectively), provides high wake losses, with almost 20% of loss after rotor, as shown in Table 5.3. It also necessary explain the non uniformity of the variation between α and y axis. The parameter α tends to have a higher percentage of variation, compared to y , as the vector moves only on its axis.

5.4

Layout Optimization: Case Study

To do this study, a Julia package called Flowfarm.jl is used, and allows to generate optimal wind farms and compare to Base Line models, obtaining the gain of the energy produced (in %) with the improved layout. In this specific case, it is used the Bastankhah Wake model [35] to calculate the wake effect. The data used to collect information of wind direction was from the period of 2020 in a region of Brazil, in Rio Grande do Norte. The parameters set to the layout of the park and the settings of wind turbines can be found in [37]

In this experiment, the aim is calculating the energy produced by the wind farm and compare the Optimized Layout with two benchmarks: (i) an evenly-spaced design (as a representative of an optimal layout if the wake effect is neglected) here-in-after named *Baseline Case*, and (ii) the actual layout of the wind farm considered in this experiment, termed *Real Case* (see Table 5.5). To do this, it is necessary to create a limited area between turbines, define a total size to the park and use a a wind distribution that takes into account the expected wind distribution for the park, as can be seen in the wind rose (Figure 5.5). Also, it was considered the yaw set point, which is adjusted to the wind speed and direction.

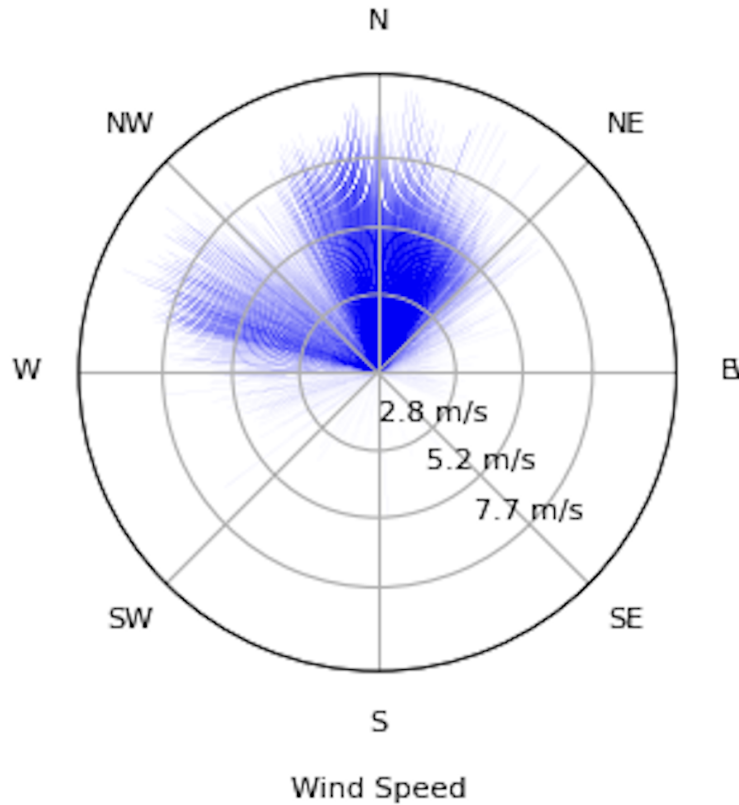


Figure 5.5: Wind Speed in Rio Grande do Norte, in the year of 2020

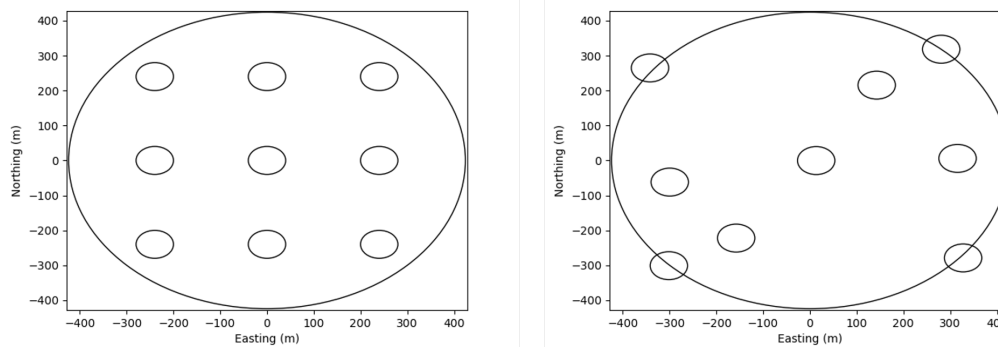


Figure 5.6: (Left) Baseline Case: An evenly spaced wind farm layout; (Right) Optimal layout changes the position of the turbines, in order to produce more energy.

Regarding the optimal design, as can be seen in Figure 5.6, it takes into account the wind speed and wind direction in the Northeast of Brazil. Furthermore, in Table 5.4 it is possible to compare the Optimal AEP with both benchmarks. Note that, by considering the layout methodology presented in this work, an improvement of roughly 15% and 1.5% were obtained with respect to the benchmarks *Baseline Case* and *Real Case*, respectively. Also, in Figure 5.6 it is possible to compare the Base Line case with the Optimal

layout. The improvement happens by the fact that the optimizer search for the layout with less wake effect as possible, taking in account the wind speed and direction. With less interruptions of the free wind, it is possible to obtain more energy in one year.

Table 5.4: AEP Comparison

	AEP (avgMW)	Improvement (%)
Baseline Case	1.14	15.21
Real Case	1.30	1.5
Optimal AEP	1.32	-

5.5

Experimental analysis and results

To conduct the analysis involving contracts and turbine positioning, the wind data from 5.2 is also taken into account. Moreover, eleven years of hourly energy prices, wind speed and direction, within the same timeframe are incorporated, as depicted in 5.7 and 5.8.

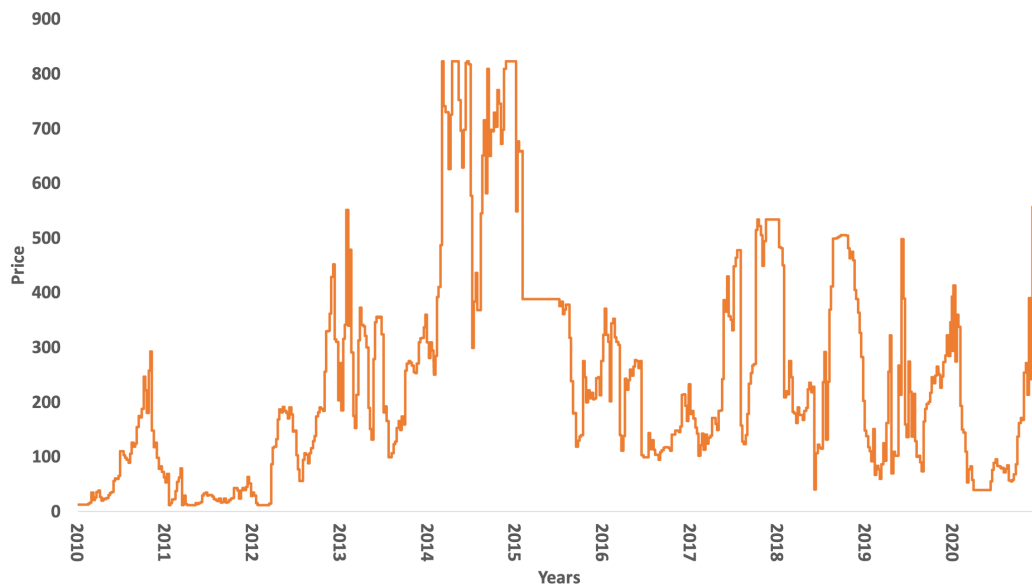


Figure 5.7: Energy prices in the Northeast of Brazil (2010 - 2020)

5.6

Baseline Analysis

In this case study, three wind farm layouts, each comprising 16 turbines, are compared. The baseline case, referred to as the "Evenly Spaced" layout, adopts a straightforward arrangement of turbines 5.9. This layout serves

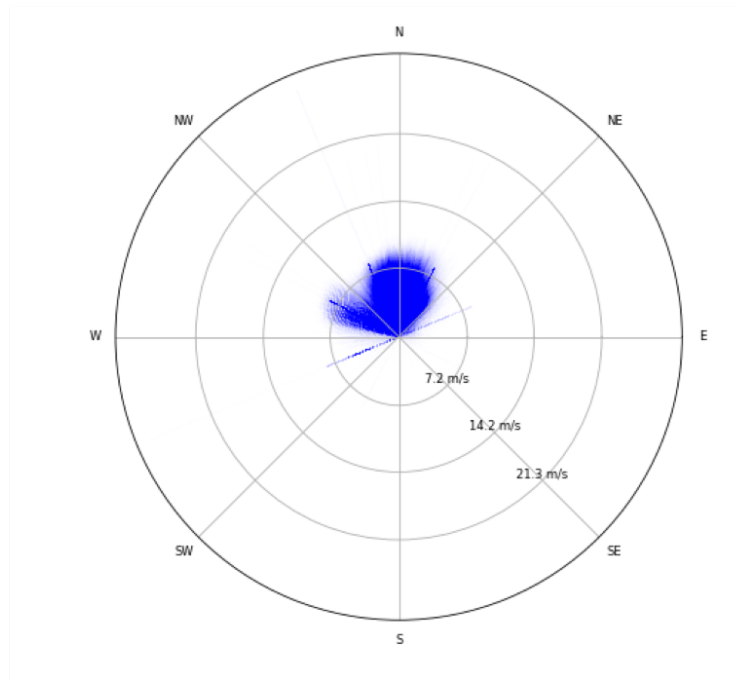


Figure 5.8: Wind Speed and Direction in Northeast, in years of 2010 - 2020

as a fundamental reference point for direct comparisons. Conversely, the "Real Case" faithfully reproduces the wind farm's actual layout, preserving the physical turbine configuration found in reality 5.10. In both cases, the Evenly Spaced and Real Case layouts are solely geared towards optimizing contracts. Lastly, the "Optimized Case" represents a scenario where the layout from the Real Case is co-optimized alongside the energy contract, as can be seen in figure 5.11, resulting in a comprehensive and integrated approach. The study's starts elucidating the default parameters, having the price of the contract as R\$ 240.00 and $\lambda = 0.5$. Given this information, Table 5.5 reveal that the benchmark case exhibits the lowest average revenue, with the Real Case following closely behind. In stark contrast, the Optimized Case achieves the highest Total Average Revenue when compared to the Evenly Spaced layout. This substantial improvement in revenue, amounting to a remarkable 22%, is attributed to the Optimized Case's superior layout, which capitalizes on favorable wind speed and direction. Consequently, this optimized configuration results in significantly increased power production for the wind farm. Furthermore, Table 5.6 provides a month-by-month breakdown of the Average Revenue, reaffirming the differences among the cases. The Evenly Spaced Case consistently records the lowest Average Revenue each month due to the suboptimal positioning of the turbines, resulting in lower hourly generation. Conversely, the Optimized Case outperforms the other cases in every month. This achievement can be attributed to the combined optimization of both the contract and the layout, leading to a significant improvement in

the park’s overall energy generation.

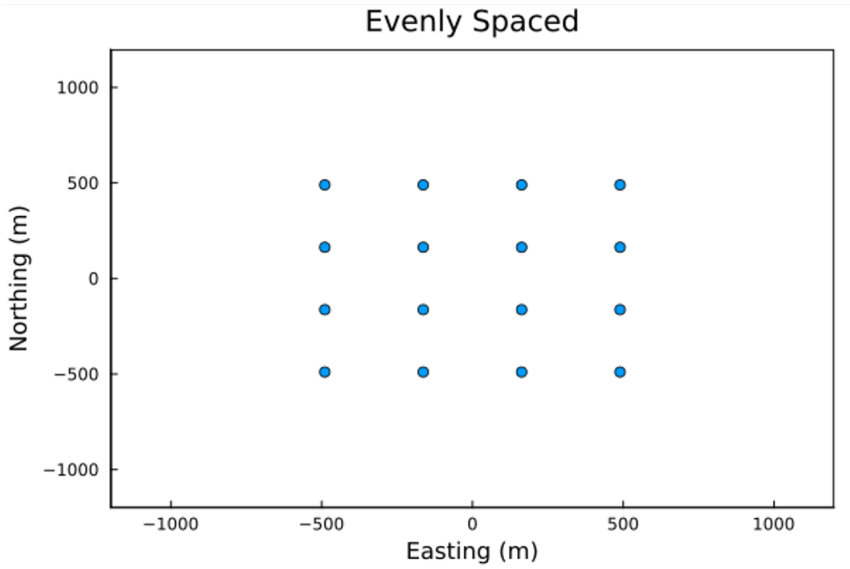


Figure 5.9: Baseline Analysis - Evenly Spaced

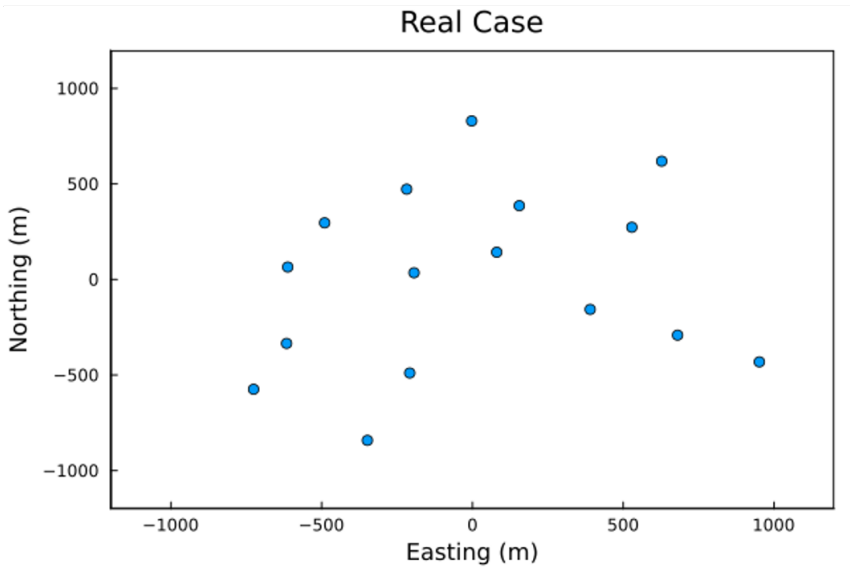


Figure 5.10: Baseline Analysis - Real Case

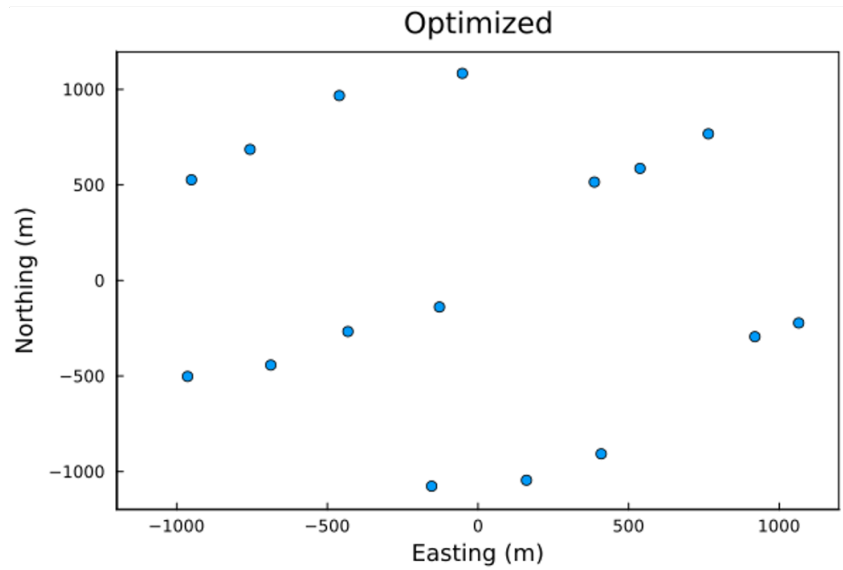


Figure 5.11: Baseline Analysis - Optimized

Table 5.5: Layout Performance Comparison

Case	Q* (% FEC)	Total Avg. Rev. (MMR\$)	Gain (%)
Baseline Case	89.1	0.61	-
Real Case	87.7	0.66	8.3
Optimized	100.0	0.74	21.3

Table 5.6: Monthly Average Revenue Table

Month	Evenly Spaced (kR\$)	Real Case (kR\$)	Optimized (kR\$)
Jan	53.10	59.14	64.56
Feb	41.49	44.93	50.22
Mar	33.49	35.57	39.61
Apr	25.41	27.26	30.97
May	29.17	31.62	36.55
Jun	36.21	36.97	44.11
Jul	44.61	44.78	52.82
Aug	61.71	61.11	72.90
Sep	63.76	70.37	81.27
Oct	77.33	89.45	100.40
Nov	70.82	78.66	84.99
Dec	68.79	76.44	82.43

Another noteworthy aspect of the analysis involves a monthly comparison between the cases. Figures 5.12 and 5.13 have been constructed as Violin Plots, providing a concise representation of the data. These visualizations are

based on the summation of daily revenue, thereby consolidating the monthly distribution.

In the plots, the left distribution represents the Optimized Case, while the right showcases a comparison between the Evenly Spaced (in blue) and Real Case (in dark red). These visualizations clearly illustrate the revenue advantage of the Optimized Case, demonstrating its superior performance compared to the other layouts. It happens by the fact of the higher generation in every month and better strategy of contracting.

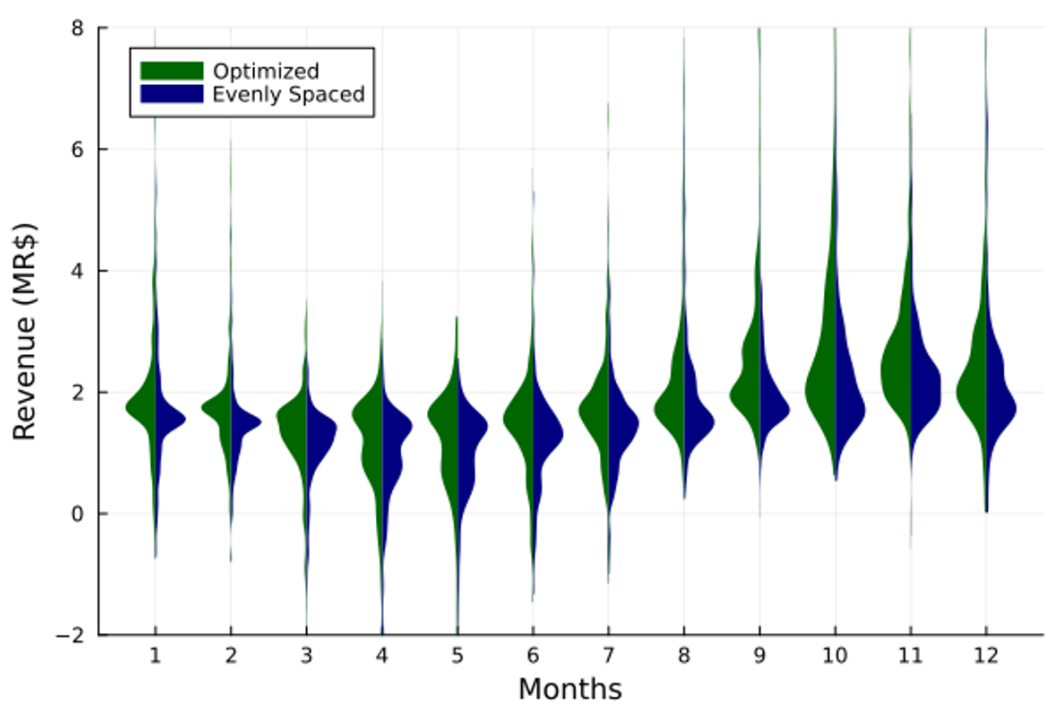


Figure 5.12: Violin Plot Distribution - Evenly Spaced

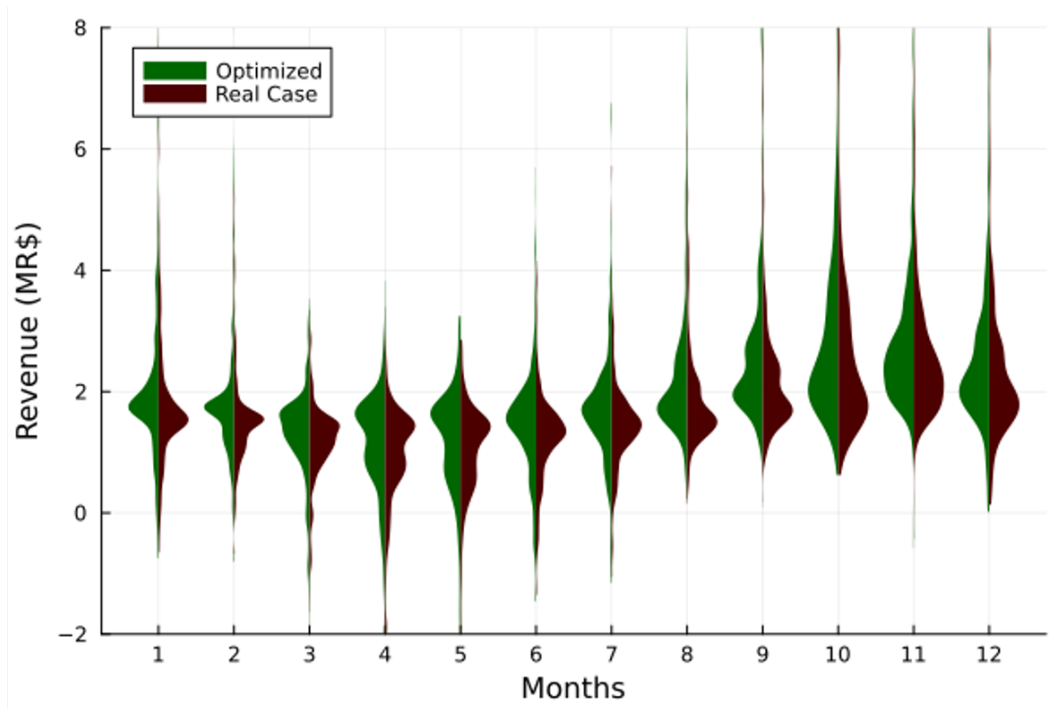


Figure 5.13: Violin Plot Distribution - Real Case

As the next step, a generation analysis will be conducted to compare the “Evenly Spaced” and “Real Case” scenarios with the “Optimized” scenario by PLD intervals. The main idea is identify the changes of the Power Production in each case. The first interval spans from R\$ 12.08 to R\$ 282.83, the second from R\$282.83 to R\$552.58, and the final interval from R\$552.58 to R\$822.83, in order to investigate the decision process of the optimizer regarding the changes in PLD.

Figures 5.14 and 5.15 show the consolidated Power Production graphs. The x axis represent the wind speed (in m/s) and the y axis, the Power Production (in MWh). These two figures presents the higher volume of power production of the Optimized case, specially when it is compared to the Evenly Spaced.

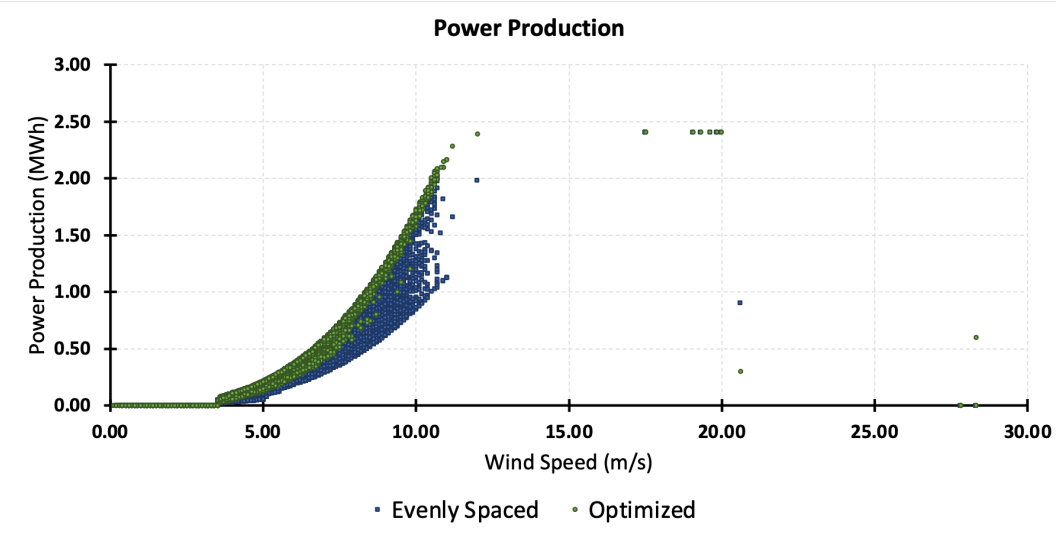


Figure 5.14: Power Production: Evenly Spaced vs Optimized

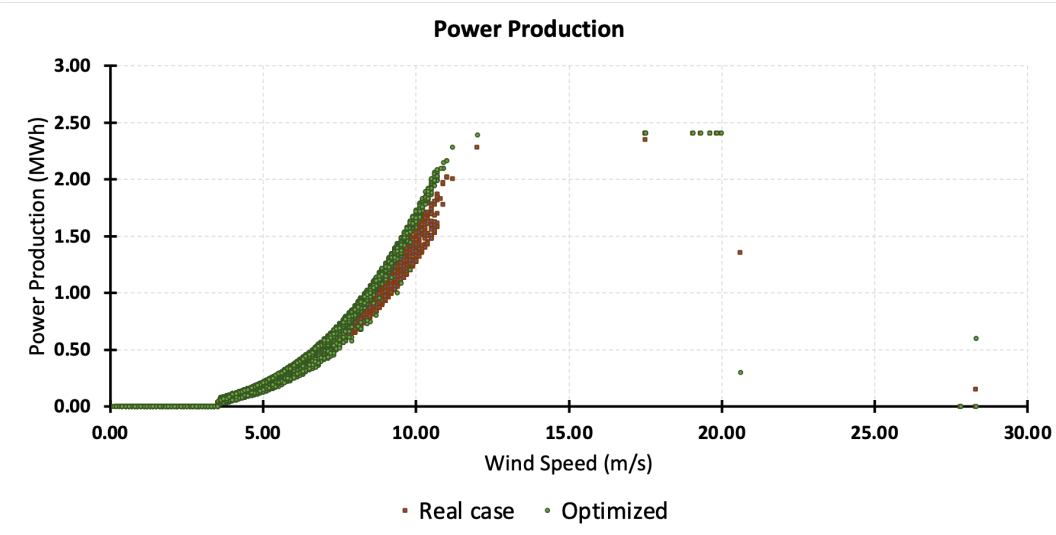


Figure 5.15: Power Production: Real Case vs Optimized

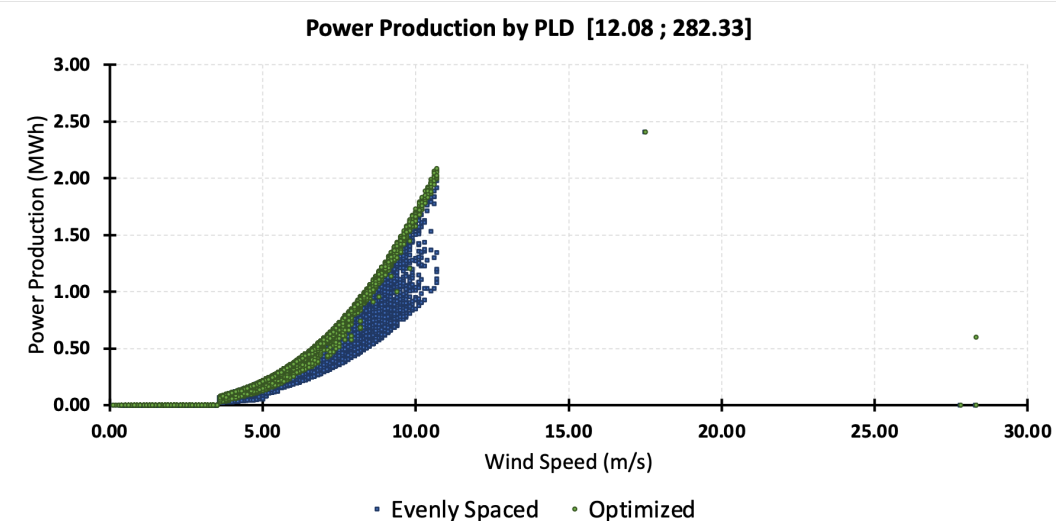


Figure 5.16: Power Production: Evenly Spaced vs Optimized - Range I

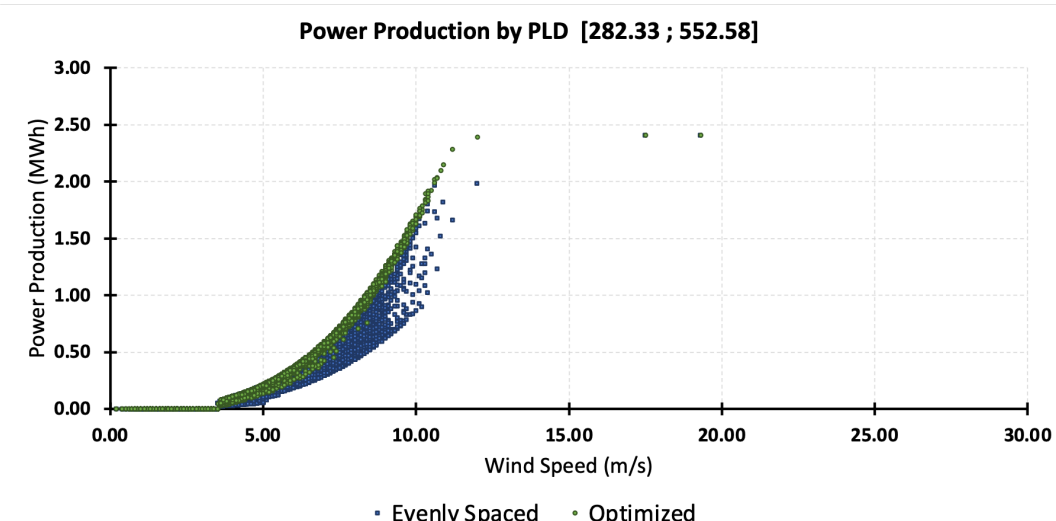


Figure 5.17: Power Production: Evenly Spaced vs Optimized - Range II

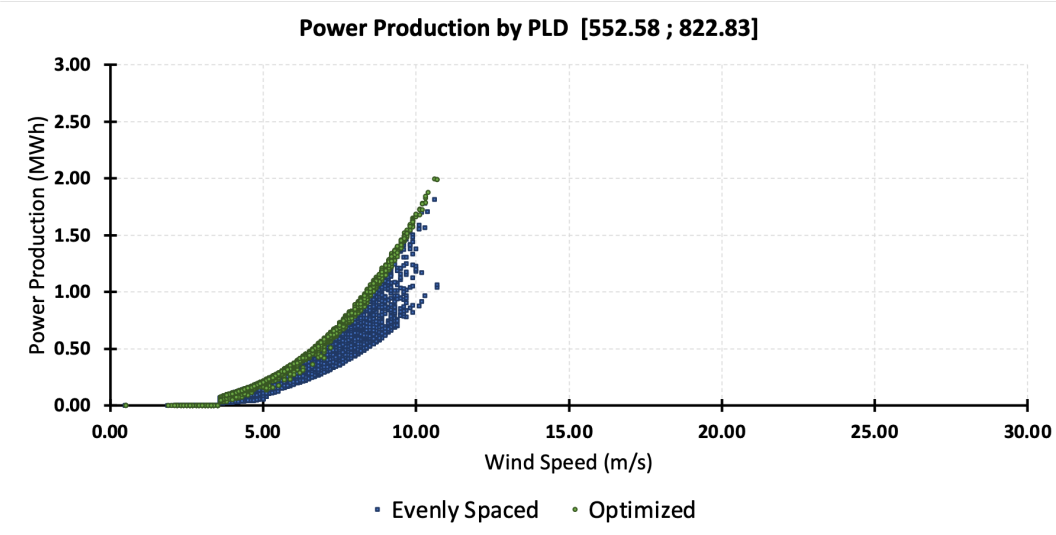


Figure 5.18: Power Production: Evenly Spaced vs Optimized - Range III

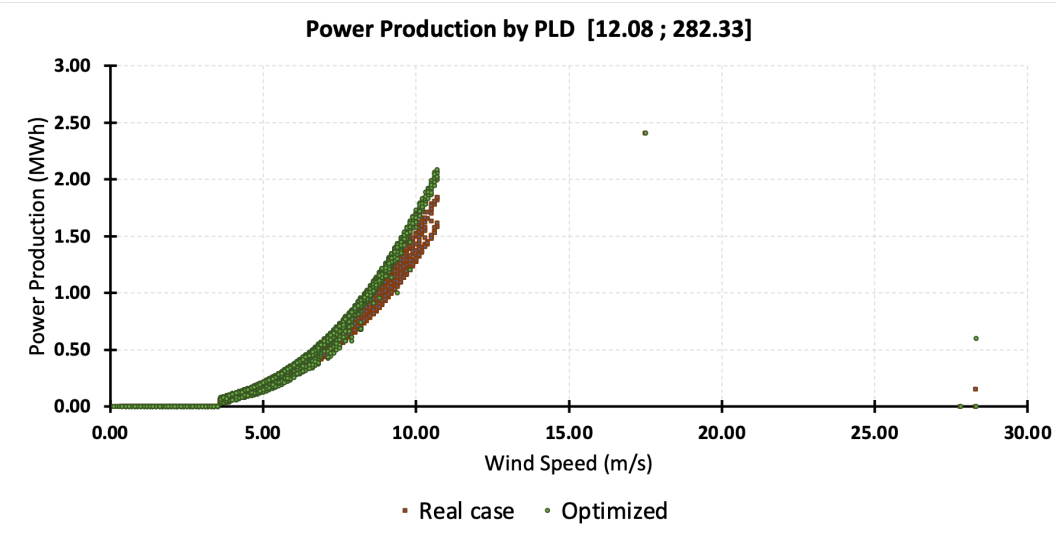


Figure 5.19: Power Production: Real Case vs Optimized - Range I

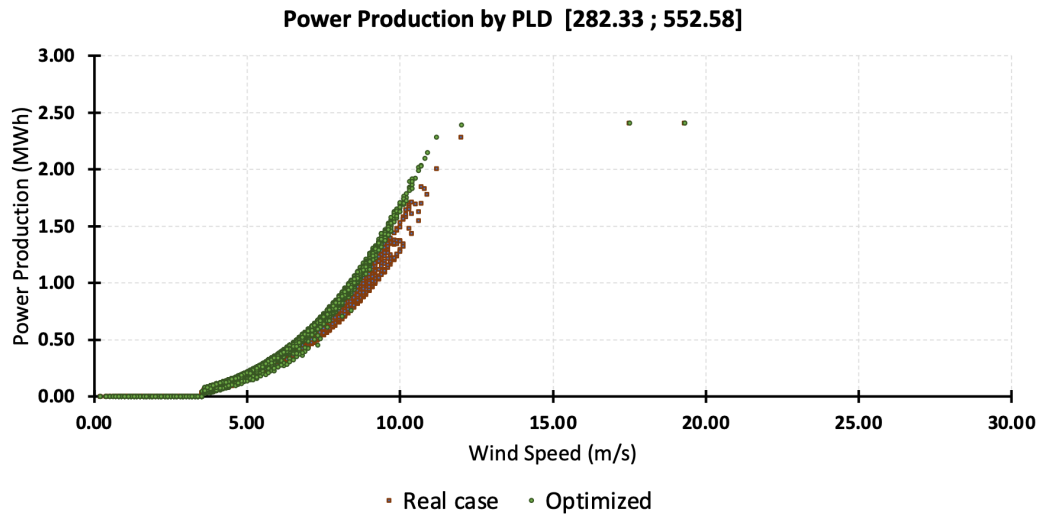


Figure 5.20: Power Production: Real Case vs Optimized - Range II

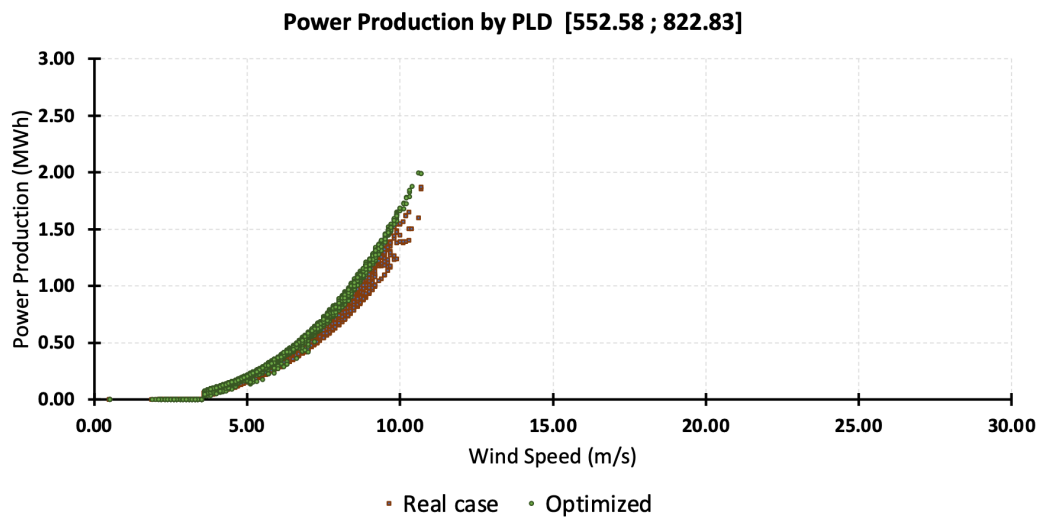


Figure 5.21: Power Production: Real Case vs Optimized - Range III

In the context of hourly energy price analysis, Figures 5.16 to 5.21 illustrate the Power Production Generation categorized by PLD, facilitating a comparative study between the Optimized, Evenly Spaced, and Real Case scenarios. These figures highlight the advantageous impact of optimal turbine positioning, as turbines are strategically located in areas with higher wind intensity, resulting in increased energy generation. Additionally, it's noteworthy to observe the differences between Figures 5.16 and 5.17, as well as Figures 5.19 and 5.20. These comparisons reveal that power production is consistently higher in periods with elevated PLD values. This underscores the co-optimization's ability to maximize power generation during times of extended high PLD conditions.

The final case study in this section examines the seasonal performance of the wind farms under consideration, comparing power production between the Optimized, Evenly Spaced, and Real Case scenarios. To begin, Figures 5.22 and 5.23 provide a comprehensive overview of the comparative analysis among the cases. As confirmed in the previous case study, the Optimized case consistently outperforms the Evenly Spaced and Real Case scenarios.

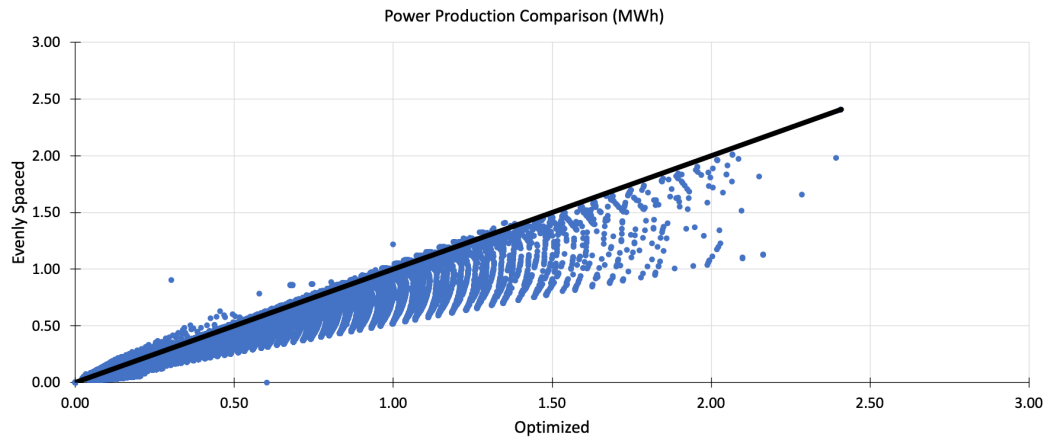


Figure 5.22: Power Production Comparison: Evenly Spaced vs Optimized

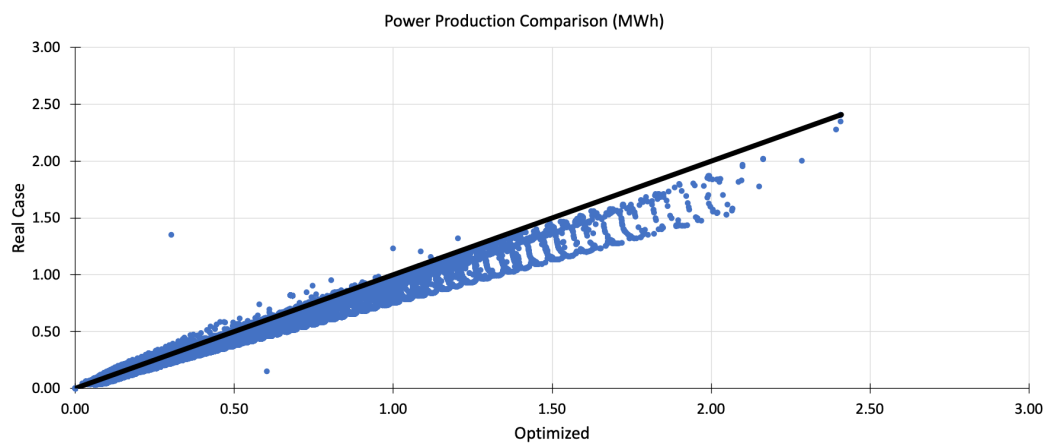


Figure 5.23: Power Production Comparison: Real Case vs Optimized

Furthermore, the findings of the seasonal study are presented. Figures 5.24, 5.25, and 5.32 through 5.33 clearly illustrate that both Spring and Winter contribute to higher power production for the park across all scenarios. This is due to increased wind exposure, resulting in enhanced energy generation as the turbines harness more wind energy.

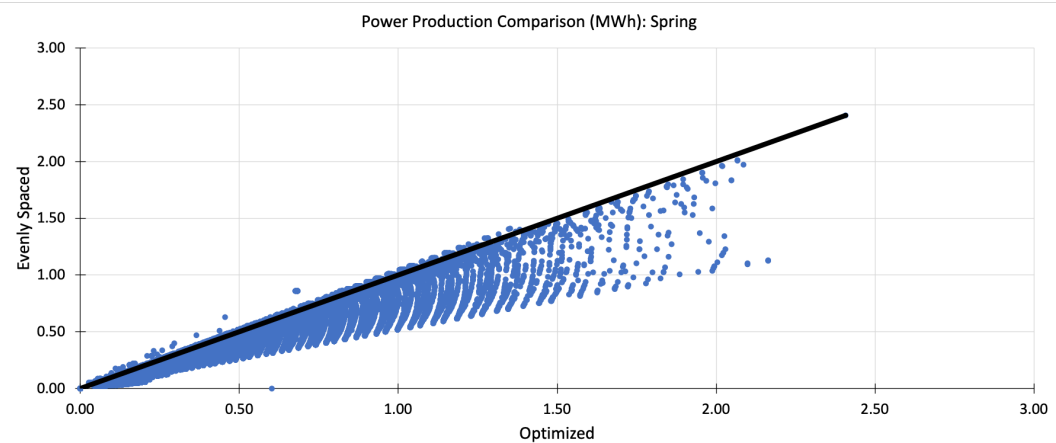


Figure 5.24: Power Production Comparison: Evenly Spaced vs Optimized - Spring.

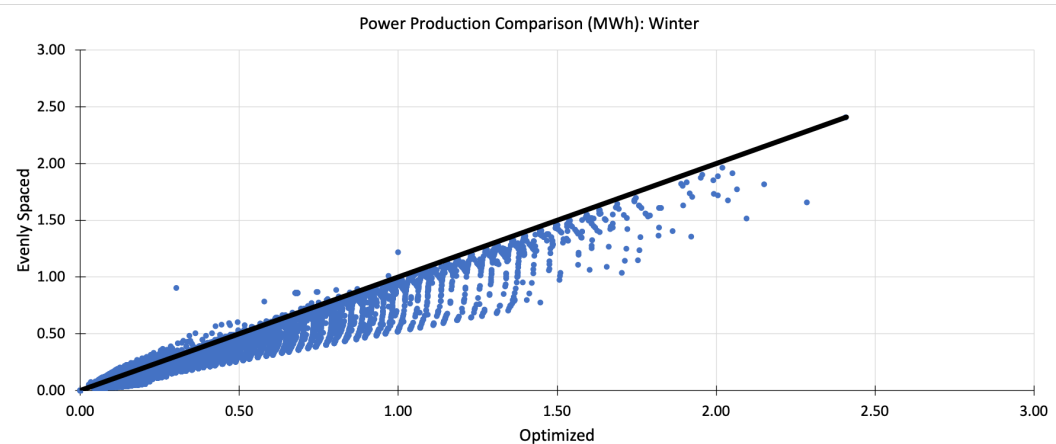


Figure 5.25: Power Production Comparison: Evenly Spaced vs Optimized - Winter.

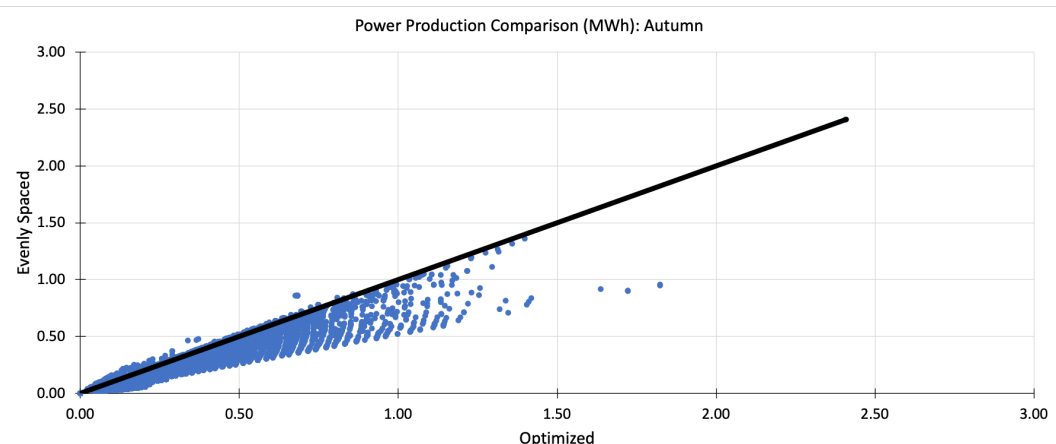


Figure 5.26: Power Production Comparison: Evenly Spaced vs Optimized - Autumn.

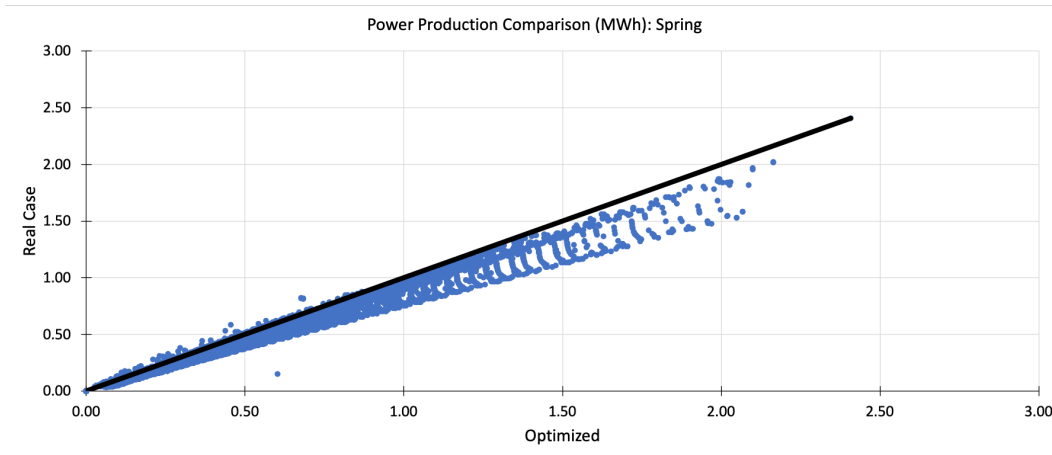


Figure 5.27: Power Production Comparison: Real Case vs Optimized - Spring.

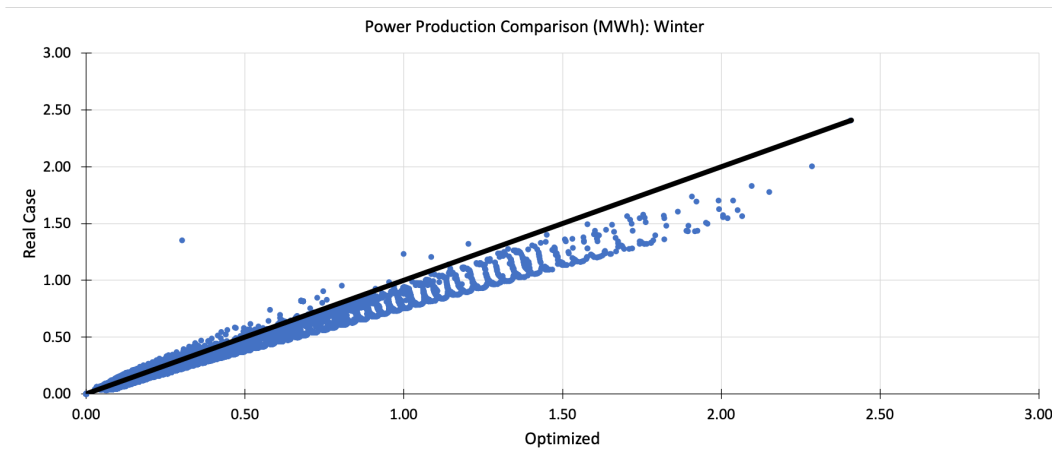


Figure 5.28: Power Production Comparison: Real Case vs Optimized - Winter.

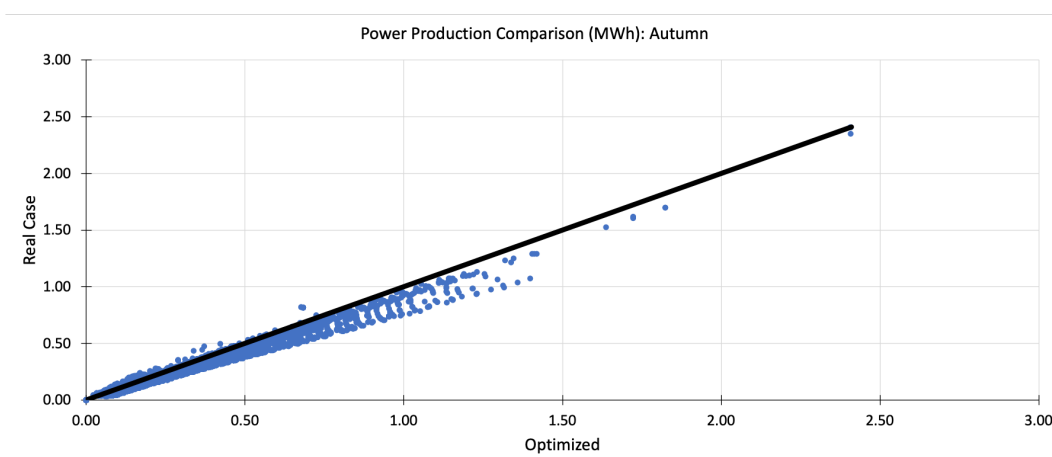


Figure 5.29: Power Production Comparison: Real Case vs Optimized - Autumn.

However, during the Summer, as observed in Figures 5.30 and 5.31, the Optimized case, while still performing well, exhibits a slightly lower increase in

power production compared to the other cases. This can be attributed to the high incidence of sunlight in the Northeast region of Brazil during this season, which results in a proportionally reduced reliance on wind energy for power generation.

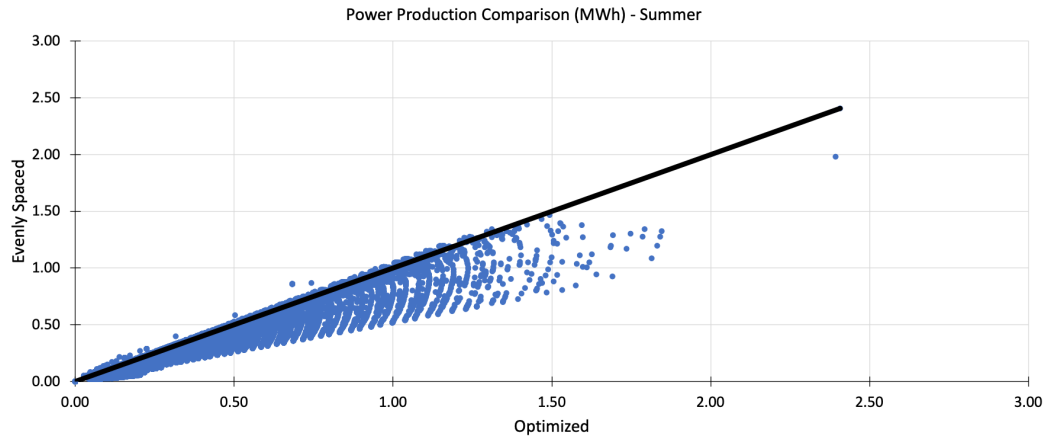


Figure 5.30: Power Production Comparison: Evenly Spaced vs Optimized - Summer.

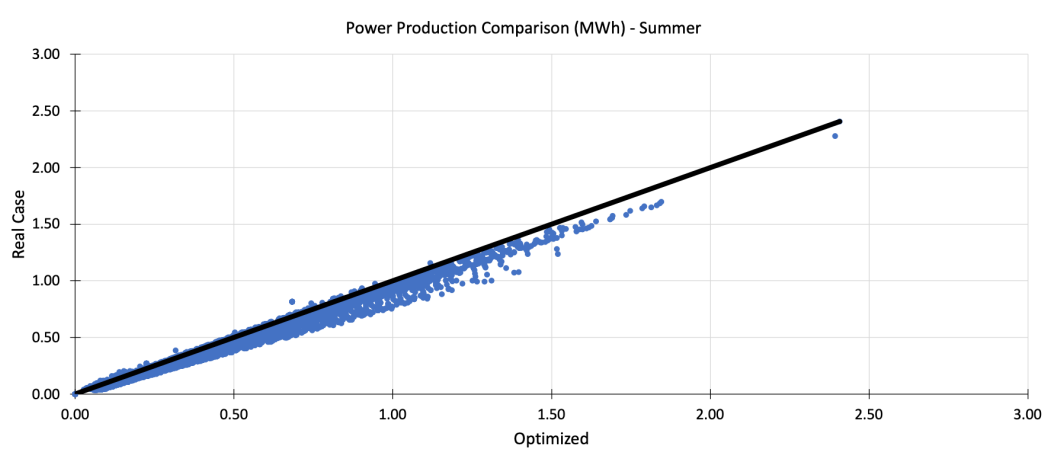


Figure 5.31: Power Production Comparison: Real Case vs Optimized - Summer.

5.7 Sensitivity Analysis

This section shifts its focus towards a sensitivity analysis involving fluctuations in contract prices. Furthermore, it delves into the influence of changes in the parameter λ , which functions as a risk regulator, on both Average Revenue and CVaR. This analysis sheds light on how agent behavior, spanning from neutral risk orientation to high risk aversion, impacts both Average Revenue and CVaR. To contextualize the risk regulator [38], it's essential to note that a λ value of 0 signifies a risk-neutral agent. Also, it

was defined that values between 0.1 and 0.3 denote a low level of risk aversion, while the range of 0.4 to 0.6 represents medium risk aversion. Finally, values between 0.7 and 0.99 indicate a highly risk-averse agent. Having established this context, the initial comparison centers on the Total Average Revenue 5.32 between the Real and Optimized cases, utilizing the same parameters as outlined in Section 5.6. It can be seen that the Optimized Case outperforms the Real Case in nearly every contract price variation. However, the scenario where the contract price is R\$ 150.00 explains the lower revenue value, offset by a considerably higher CVaR as can be observed in figure 5.33. This indicates that the agent is prioritizing risk mitigation over potential losses in this specific context. Finally, the comparison of the Optimal Contract Amount (% FEC) is presented in figure 5.34. The trend indicates that as the contract price increases, the agent tends to contract a larger percentage of energy. This suggests that having a fixed contract with a higher value is more favorable than relying on spot prices. Additionally, when comparing the evolution of the FEC between the Optimized and Real Cases, it becomes evident that the agent in the Optimized case consistently maintains a higher level of contractual commitment compared to the Real Case.

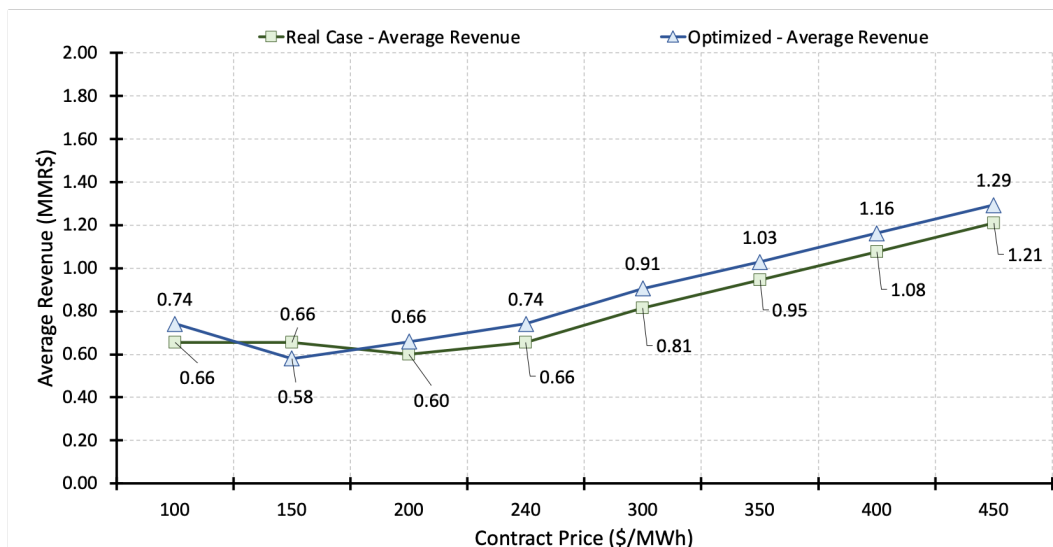


Figure 5.32: Contract Variation - Total Average Revenue: Real Case vs Optimized.

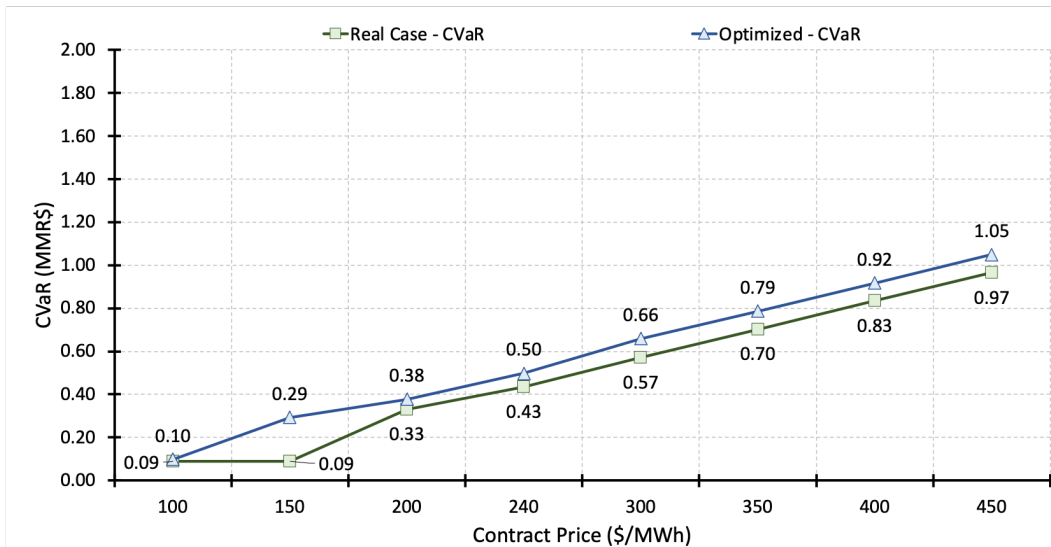


Figure 5.33: Contract Variation - CVaR: Real Case vs Optimized.

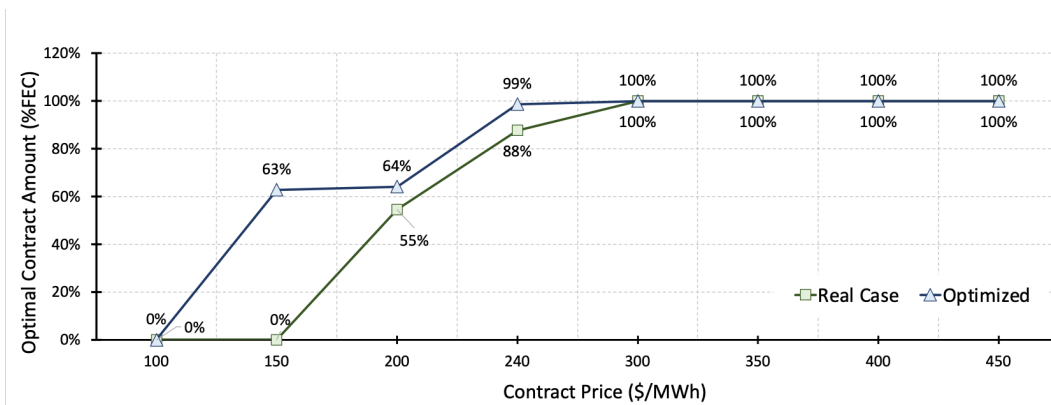


Figure 5.34: Contract Variation - %FEC: Real Case vs Optimized.

The final analysis within this section examines variations in the parameter λ . In this instance, the contract price is fixed at R\$ 185.00. Figures 5.38 and 5.39 illustrate the complementary relationship between Total Average Revenue and CVaR. Lower values of λ tend to correspond to higher Revenue figures, while the worst-case scenario becomes more pronounced as the risk regulator increases. Notably, starting at $\lambda = 0.75$, Revenue values remain relatively consistent until the final value of $\lambda = 0.99$. An observation emerges when Revenue at $\lambda = 0.75$ is R\$ 200,000.00 lower than in the case with $\lambda = 0.8$. This phenomenon can be attributed to co-optimization altering the layout configuration. Different layouts can suggest varying energy production levels, thus resulting in divergent revenue outcomes. Finally, Figure 5.37 elucidates the agent's contracting behavior. It is evident that low λ values represent neutral risk-takers, leading to low (or zero) contract values. In contrast, higher values of λ represent 50% to 70% of the total revenue.

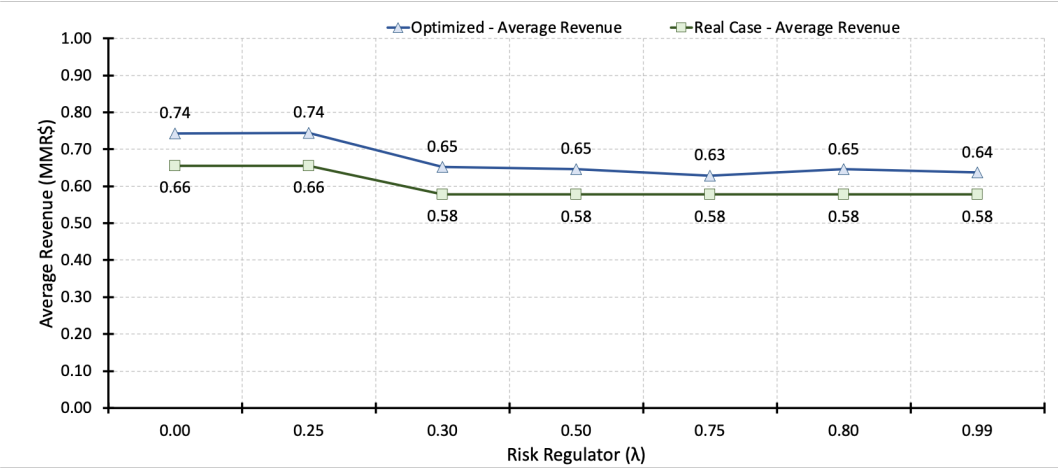


Figure 5.35: λ Variation - Total Average Revenue: Real Case vs Optimized.

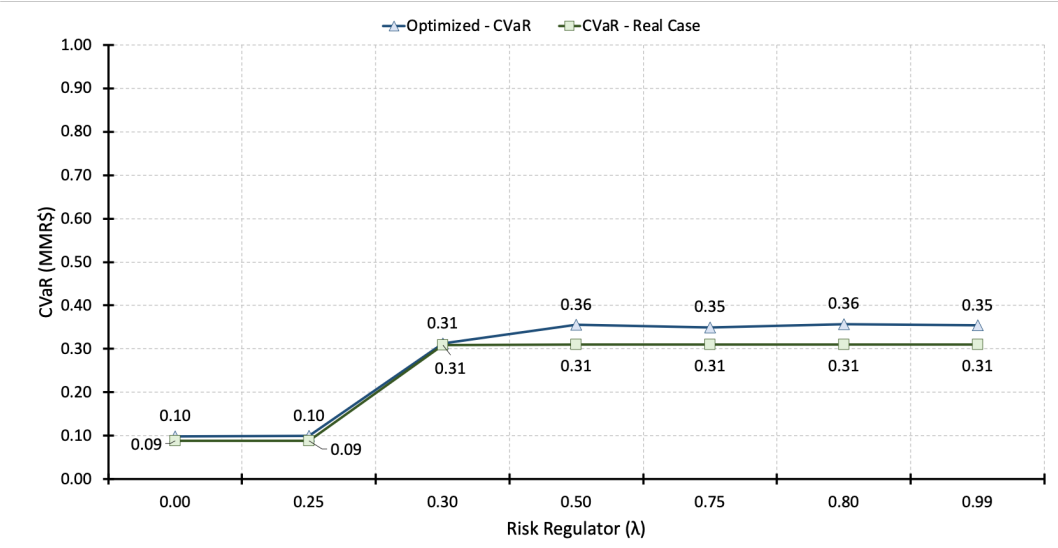


Figure 5.36: λ Variation - CVaR: Real Case vs Optimized.

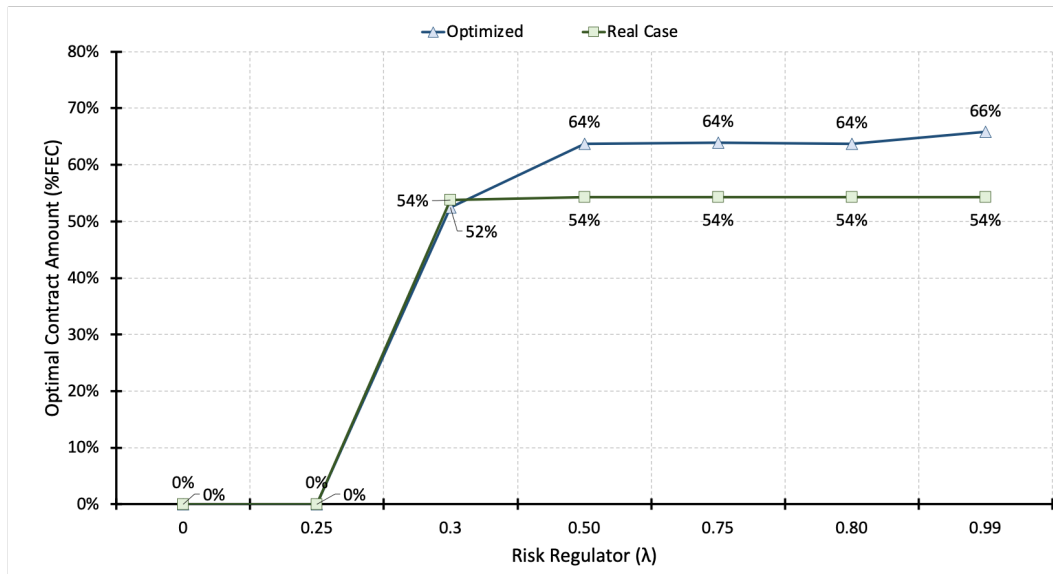


Figure 5.37: λ Variation - %FEC: Real Case vs Optimized.

5.8

Analysis over current practices

The final section of the case study aims to compare the Optimized layout with a case referred to as the 'Sequential Case.' In this scenario, the Evenly Spaced case undergoes layout optimization first, followed by the contract optimization process. Subsequently, this two-step optimized case is compared to the co-optimized case, where all decision variables are optimized simultaneously. The objective is to simulate the construction of a wind park and gain insights into which modeling approach is more effective for the study. Contract values were set at R\$ 240.00 and λ was fixed at 0.4. As depicted in Table 5.7, noticeable differences in contract allocation and Total Average Revenue exist between the Sequential and Optimized cases. This disparity can be attributed to the higher efficiency of co-optimization, which optimizes all decision variables together. Additionally, the layouts differ (5.38 and 5.39), leading to variations in power generation. The Revenue improvement, as shown in the last column, reaches 3%, favoring the co-optimized model.

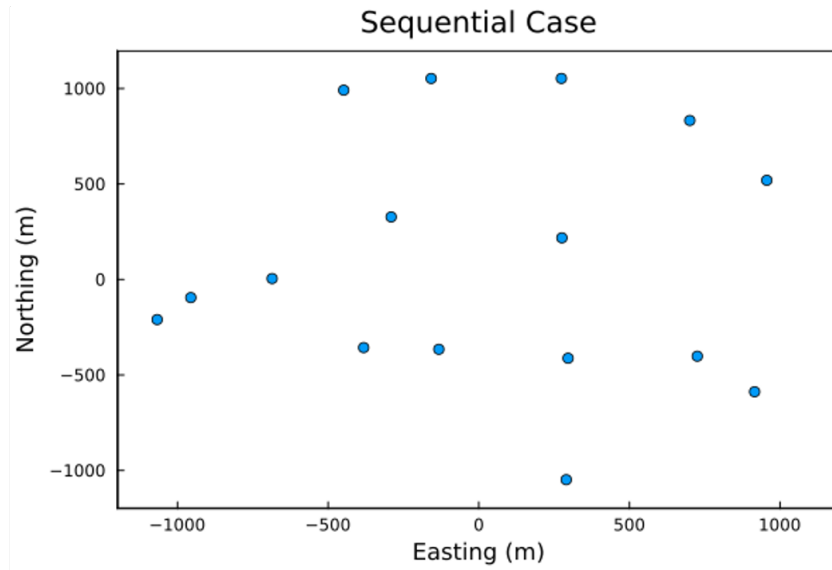


Figure 5.38: Sequential Layout with contract cost = R\$240.00 and $\lambda = 0.4$.

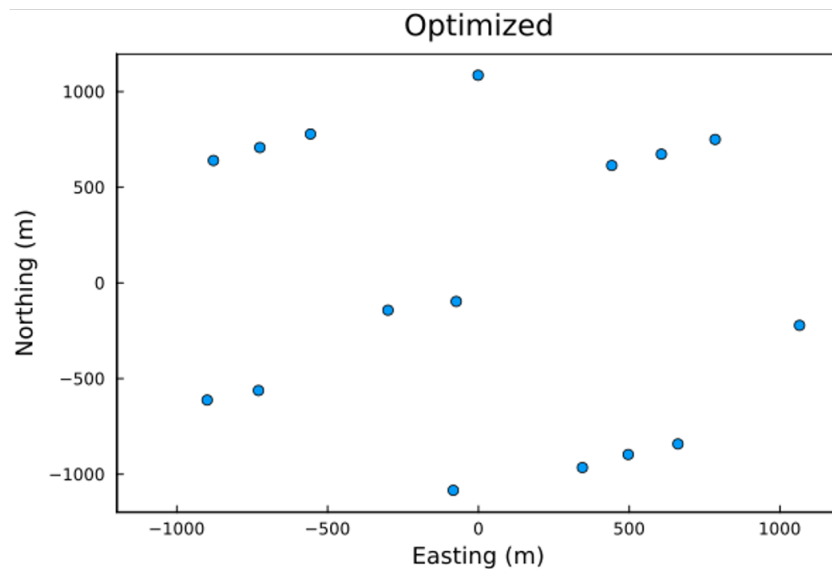


Figure 5.39: Optimal Layout with contract cost = R\$240.00 and $\lambda = 0.4$.

Table 5.7: Layout Performance Comparison

Case	Q* (% FEC)	Total Avg. Revenue (kR\$)	Gain (%)
Sequential	97.13	720.79	-
Optimized	100.0	742.91	3.1

Another noteworthy comparison is the monthly revenue of both cases, as shown in Table 5.8. The Optimized case consistently outperforms the Sequential case in every month of the year.

Table 5.8: Average Revenue Comparison

Month	Sequential (kR\$)	Optimized (kR\$)	Gain (%)
Jan	63.03	64.81	2.8
Feb	49.21	50.34	2.3
Mar	38.94	39.77	2.1
Apr	30.25	31.00	2.5
May	35.52	36.61	3.1
Jun	42.50	44.15	3.9
Jul	51.30	52.87	3.1
Aug	70.66	72.90	3.2
Sep	78.69	81.22	3.2
Oct	97.21	100.50	3.4
Nov	82.97	85.64	3.2
Dec	80.51	83.10	3.2

Overall, this analysis demonstrates the pivotal role of co-optimization in enhancing the profitability and operational efficiency of wind farms, offering valuable insights for decision-makers in the renewable energy sector.

6

Conclusions

This work has offered a comprehensive exploration of wind farm optimization from multiple angles, providing a holistic perspective on how layout configurations, contract allocation, risk aversion, seasonal influences, and co-optimization strategies intersect and influence the profitability and operational efficiency of wind farms. As the world confronts the pressing issue of climate change, wind power stands out as a critical source of clean energy. However, realizing its full potential relies on the optimization of wind farm layouts, particularly in light of the complex wake effect. This dissertation delves into Wind Farm Layout Optimization (WFLO) using the Bastankhah Wake Model and the scope of this study goes beyond layout design; it encompasses the intricate task of mitigating the wake effect's impact along with the seek for a risk-averse-value maximizing trading strategy. To account for risk-averseness, a combination between Expected Value and the left-side-quantile-based risk-measure functionals, the Conditional Value-at-Risk (CVaR) measure were built. To support this research, an open-source package `OptimalLayout.jl` was developed, in order to co-optimize the positioning of wind turbines to mitigate wake effect impact, and the contracting strategy of a Risk-Averse agent/generator. Through a series of practical case studies across diverse dynamic environments, this research illustrates the real-world applicability of WFLO. Also, these investigations intricately examine its influence on power production and revenue dynamics, offering valuable insights into sustainable energy solutions.

Three case studies of a wind farm in Northeast Brazil assess the impact of layout optimization on power production. First, an in-depth analysis of the annual energy generation achieved by an optimized model were presented. The second case involves a revenue comparison using a benchmark model, where turbine coordinates and contracts are optimized, and the sensitivity of contract pricing and risk regulation parameters is analyzed. Lastly, the co-optimized instance were contrasted with the process of sequential optimization for a comprehensive assessment. These findings not only contribute to the growing body of knowledge in renewable energy but also provide actionable insights for stakeholders and decision-makers in the wind energy sector. Ultimately, this research underscores the critical role of optimization in advancing the sustainability and economic viability of wind energy projects.

7

References

- [1] ON CLIMATE CHANGE, I. P.. **Climate change 2021: The physical science basis. contribution of working group i to the sixth assessment report of the intergovernmental panel on climate change.** 2021. 1
- [2] FRIEDLINGSTEIN, P.; O'SULLIVAN, M.; JONES, M. W.; ANDREW, R. M.; HAUCK, J.; PETERS, G. P.; PETERS, W.; PONGRATZ, J.; SITCH, S.; LE QUÉRÉ, C. ; OTHERS. **Global carbon budget 2021.** Earth System Science Data, 2021. 1
- [3] COUNCIL, G. W. E.. **Global wind report 2021.** Global Wind Energy Council (GWEC), 2021. 1
- [4] AGENCY, I. R. E.. **Renewable energy statistics 2022.** International Renewable Energy Agency (IRENA), 2022. 1
- [5] GEBRAAD, P.; THOMAS, J. J.; NING, A.; FLEMING, P. ; DYKES, K.. **Maximization of the annual energy production of wind power plants by optimization of layout and yaw-based wake control.** Wind Energy, 20(1):97–107, 2017. 1
- [6] PADRÓN, A. S.; THOMAS, J.; STANLEY, A. P. J.; ALONSO, J. J. ; NING, A.. **Polynomial chaos to efficiently compute the annual energy production in wind farm layout optimization.** Wind Energy Science, 4:211–231, May 2019. 1
- [7] THOMAS, J. J.; BAKER, N. F.; MALISANI, P.; QUAEGHEBEUR, E.; PEREZ-MORENO, S. S.; JASA, J.; BAY, C.; TILLI, F.; BIENIEK, D.; ROBINSON, N.; STANLEY, A. P. J.; HOLT, W. ; NING, A.. **A comparison of eight optimization methods applied to a wind farm layout optimization problem.** Wind Energy Science, 8(5):865–891, Apr. 2023. 1
- [8] STANLEY, A. P. J.; NING, A.. **Massive simplification of the wind farm layout optimization problem.** Wind Energy Science, 4(4):663–676, Dec. 2019. 1
- [9] THOMAS, J. J.; BAY, C. J.; STANLEY, A. P. J. ; NING, A.. **Gradient-based wind farm layout optimization results compared with large-eddy simulations.** Wind Energy Science, Jan. 2022. (in review). 1

- [10] STANLEY, A. P. J.; NING, A. ; DYKES, K.. **Optimization of turbine design in wind farms with multiple hub heights, using exact analytic gradients and structural constraints.** *Wind Energy*, 22(5):605–619, May 2019. 1
- [11] KIRCHNER-BOSSI, N.; PORTÉ-AGEL, F.. **Realistic wind farm layout optimization through genetic algorithms using a gaussian wake model.** *Energies*, 11(12), 2018. 1
- [12] STANLEY, A. P.; KING, J.; BAY, C. ; NING, A.. **A model to calculate fatigue damage caused by partial waking during wind farm optimization.** *Wind Energy Science*, 7(1):433–454, Mar. 2022. 1
- [13] TINGEY, E.; NING, A.. **Development of a parameterized reduced-order vertical-axis wind turbine wake model.** *Wind Engineering*, June 2019. 1
- [14] BÖHME, G. S.; FADIGAS, E. A.; GIMENES, A. L. ; TASSINARI, C. E.. **Wake effect measurement in complex terrain - a case study in brazilian wind farms.** *Energy*, 161:277–283, 2018. 1
- [15] BASTIAN-PINTO, C. L.; ARAUJO, F. V. D. S.; BRANDÃO, L. E. ; GOMES, L. L.. **Hedging renewable energy investments with bitcoin mining.** *Renewable and Sustainable Energy Reviews*, 138:110520, 2021. 1
- [16] PAN, K.; GUAN, Y.. **Integrated stochastic optimal self-scheduling for two-settlement electricity markets.** *INFORMS Journal on Computing*, 34(3):1819–1840, 2022. 1
- [17] MUNHOZ, F. C.. **Two-settlement system for the brazilian electricity market.** *Energy Policy*, 152:112234, 2021. 1
- [18] FÂNZERES, B.; STREET, A.. **Cálculo da curva de disposição a contratar de geradores hidrelétricos: Uma abordagem robusta ao preço de curto-prazo.** XXI SNPTEE, 2011. 1
- [19] FANZERES, B.; AHMED, S. ; STREET, A.. **Robust strategic bidding in auction-based markets.** *European Journal of Operational Research*, 272(3):1158–1172, 2019. 1
- [20] FÂNZERES, B.; STREET, A.; LIMA, D.; VEIGA, Á.; FREIRE, L. ; AMARAL, B.. **Comercialização de energia eólica no ambiente livre: Desafios e soluções inovadoras.** XII Simpósio de especialistas em planejamento da operação e expansão elétrica, 2012. 1

- [21] ARANHA, A. S.; STREET, A.; FERNANDES, C. ; GRANVILLE, S.. **Risk-constrained optimal dynamic trading strategies under short- and long-term uncertainties**. IEEE Transactions on Power Systems, 38(2):1474–1486, 2023. 1
- [22] STREET, A.; BARROSO, L. A.; FLACH, B.; PEREIRA, M. V. ; GRANVILLE, S.. **Risk constrained portfolio selection of renewable sources in hydrothermal electricity markets**. IEEE Transactions on Power Systems, 24(3):1136–1144, 2009. 1
- [23] BRIGATTO, A.; FANZERES, B.. **A soft robust methodology to devise hedging strategies in renewable energy trading based on electricity options**. Electric Power Systems Research, 207:107852, 2022. 1
- [24] NETO, D. P.; DOMINGUES, E. G.; COIMBRA, A. P.; DE ALMEIDA, A. T.; ALVES, A. J. ; CALIXTO, W. P.. **Portfolio optimization of renewable energy assets: Hydro, wind, and photovoltaic energy in the regulated market in brazil**. Energy Economics, 64:238–250, 2017. 1
- [25] STREET, A.; LIMA, D. A.; VEIGA, Á.; FÂNZERES, B.; FREIRE, L. ; AMARAL, B.. **Fostering wind power penetration into the brazilian forward-contract market**. p. 1–8, 2012. 1
- [26] BASTANKHAH, M.; PORTÉ-AGEL, F.. **A new analytical model for wind-turbine wakes**. Renewable energy, 70:116–123, 2014. 1, 2
- [27] JENSEN, N. O.. **A note on wind generator interaction**, volumen 2411. Citeseer, 1983. 1, 2.1
- [28] PAPI, F.; BALDUZZI, F.; FERRARA, G. ; BIANCHINI, A.. **Uncertainty quantification on the effects of rain-induced erosion on annual energy production and performance of a multi-mw wind turbine**. Renewable Energy, 165:701–715, 2021. 2
- [29] VAN DER LAAN, M.; ANDERSEN, S.; RÉTHORÉ, P.-E.; BAUNGAARD, M.; SØRENSEN, J. ; TROLDBORG, N.. **Faster wind farm aep calculations with cfd using a generalized wind turbine model**. In: JOURNAL OF PHYSICS: CONFERENCE SERIES, volumen 2265, p. 022030. IOP Publishing, 2022. 2
- [30] TENNEKES, H.; LUMLEY, J. L.; LUMLEY, J. L. ; OTHERS. **A first course in turbulence**. MIT press, 1972. 2.1

- [31] BURTON, T.; JENKINS, N.; SHARPE, D. ; BOSSANYI, E.. **Wind energy handbook**. John Wiley & Sons, 2011. 2.1
- [32] BAKER, N. F.; STANLEY, A. P.; THOMAS, J. J.; NING, A. ; DYKES, K.. **Best practices for wake model and optimization algorithm selection in wind farm layout optimization**. In: AIAA SCITECH 2019 FORUM, p. 0540, 2019. 2.1
- [33] FRANDBSEN, S.; BARTHELMIE, R.; PRYOR, S.; RATHMANN, O.; LARSEN, S.; HØJSTRUP, J. ; THØGERSEN, M.. **Analytical modelling of wind speed deficit in large offshore wind farms**. *Wind Energy: An International Journal for Progress and Applications in Wind Power Conversion Technology*, 9(1-2):39–53, 2006. 2.1
- [34] JIMÉNEZ, Á.; CRESPO, A. ; MIGOYA, E.. **Application of a les technique to characterize the wake deflection of a wind turbine in yaw**. *Wind energy*, 13(6):559–572, 2010. 2.2
- [35] BASTANKHAH, M.; PORTÉ-AGEL, F.. **Experimental and theoretical study of wind turbine wakes in yawed conditions**. *Journal of Fluid Mechanics*, 806:506–541, 2016. 2.2, 5.4
- [36] ROCKAFELLAR, R. T.; URYASEV, S.. **Conditional Value-at-Risk for General Loss Distributions**. *Journal of Banking & Finance*, 26(7):1443–1471, July 2002. 3.2
- [37] THOMAS, J. J.; MCOMBER, S. ; NING, A.. **Wake expansion continuation: Multi-modality reduction in the wind farm layout optimization problem**. *Wind Energy*, 25(4):678–699, 2022. 5.4
- [38] FANZERES, B.; STREET, A. ; BARROSO, L. A.. **Contracting Strategies for Generation Companies with Ambiguity Aversion on Spot Price Distribution**. XVIII Power System Computational Conference (XVIII PSCC) 2014, p. 1–8, Aug. 2014. 5.7